uOttawa

L'Université canadienne
Canada's university

FACULTÉ DES ÉTUDES SUPÉRIEURES ET POSTOCTORALES

uOttawa

L'Université canadienne
Canada's university

FACULTY OF GRADUATE AND POSDOCTORAL STUDIES

Amir Jabri

AUTEUR DE LA THÈSE / AUTHOR OF THESIS

M.Sc. (Chemistry)

GRADE / DEGREE

Department of Chemistry

FACULTÉ, ÉCOLE, DÉPARTEMENT / FACULTY, SCHOOL, DEPARTMENT

Mechanism and Ligand Design in Ruthenium Catalysis

TITRE DE LA THÈSE / TITLE OF THESIS

D. Fogg

DIRECTEUR (DIRECTRICE) DE LA THÈSE / THESIS SUPERVISOR

CO-DIRECTEUR (CO-DIRECTRICE) DE LA THÈSE / THESIS CO-SUPERVISOR

EXAMINATEURS (EXAMINATRICES) DE LA THÈSE / THESIS EXAMINERS

S. Barry

D. Richeson

Gary W. Slater

LE DOYEN DE LA FACULTÉ DES ÉTUDES SUPÉRIEURES ET POSTDOCTORALES /
DEAN OF THE FACULTY OF GRADUATE AND POSTDOCORAL STUDIES

MECHANISM AND LIGAND DESIGN IN RUTHENIUM CATALYSIS

By

AMIR JABRI

Thesis submitted to the
Faculty of Graduate and Postdoctoral Studies
University of Ottawa
In partial fulfillment of the requirements for the degree of

Master of Science

Ottawa-Carleton Chemistry Institute
University of Ottawa
Ottawa, Ontario
Canada

Your file Votre référence
ISBN: 0-494-15072-6
Our file Notre référence
ISBN: 0-494-15072-6

ABSTRACT

The known ruthenium pincer complex $RuCl(\eta^3\text{-dcpx})(PPh_3)$ (**7**) (PCP = η^3-2,6-$(PCy_2CH_2)_2C_6H_3$) was transformed into several different hydride products under standard transfer hydrogenation conditions. In situ ^{31}P NMR analysis during thermolysis of **7** in basic isopropanol permitted identification of $RuH(\eta^3\text{-dcpx})(PPh_3)(N_2)$ (**8a/b**), $RuH(\eta^3\text{-dcpx})(PPh_3)$ (**10**), and $RuH(\eta^3\text{-dcpx})(PPh_3)(H_2)$ (**9a/b**). A spectroscopically unobservable species, $Ru(H)_2[\eta^2\text{-PC(H)P}]$ (**12**), is proposed as the active species in transfer hydrogenation catalysis. The novel precatalyst, $RuCl(\eta^3\text{-dcpx})(py)_2$ (**14**), which may provide a more active catalyst, was synthesized and characterized.

Routes were explored to chelating monoanionic ligands containing a pyrrole group functionalized with N-heterocyclic carbene donors. The imidazolium salts were synthesized and characterized by NMR, IR, and mass spectrometry. Attempts to make transition metal complexes of these ligands were unsuccessful due to facile isomerization under the basic conditions required to form the free carbenes, and oxidation of the ligands in the presence of ruthenium(II), silver(I), and palladium(II) precursors.

Several primary and secondary phosphine complexes of ruthenium were synthesized and tested for their activity in catalytic transfer hydrogenation. Of these, only the bulky $HPCy_2$ ligand in $RuCl_2(HPCy_2)_4$ (**18a/b**) provided high catalytic activity. Reaction of $RuCl_2(PCy_3)_2(=CHPh)$ (**24**) with $HPCy_2$ transforms it cleanly to **18a**, potentially opening new opportunities in tandem catalysis.

TABLE OF CONTENTS

LIST OF ABBREVIATIONS

atm	atmosphere (1 atm = 760 mmHg, 101.3 kPa, 14.696 psi)
br	broad
c-	cis
$^{13}C\{^{1}H\}$	proton-decoupled carbon-13 (NMR)
Cy	cyclohexyl
d	doublet
dcpx	1,3-bis[(dicyclohexylphosphanyl)-methyl]-benzene
dcpyb	1,4-bis(dicyclohexylphosphino)butane
DEPT	Distortionless Enhancement by Polarization Transfer
DMF	N,N-dimethylformamide
dmso	dimethylsulfoxide
ESI	Electro Spray Ionization (mass spectrometry)
HMBC	Heteronuclear Multiple Bond Coherence
HMQC	Heteronuclear Multiple Quantum Coherence
Hz	Hertz, cycles per second
IMes	bis(1,3-(2,4,6-trimethylphenyl)imidazol-2-ylidene
IR	Infrared
J	coupling constant, in Hz
L	ligand
LAH	lithium aluminum hydride

λ	wavelength
M	central metal atom in a complex
m	multiplet (NMR)
m	meta
NN^{i}	2-[(2,6-diisopropylphenyl)imino)pyrrolide
NHC	N-heterocyclic carbene
NMR	Nuclear Magnetic Resonance
o	ortho
$^{31}P\{^{1}H\}$	proton-decoupled phophorus-31 (NMR)
PP	chelating ditertiary phosphine ligand
py	pyridine
pyr	pyrrole
q	quartet (NMR)
RT	room temperature
s	singlet (NMR)
t	triplet (NMR)
tert-, ^{t}	tertiary
t	trans
THF	tetrahydrofuran
TOF	mol substrate x mol catalyst^{-1} x h^{-1}
T_1	longitudinal relaxation time (NMR)
XRD	X-Ray Diffraction

δ	chemical shift (in ppm)
ν	frequency (in cm^{-1})
η	hapticity
μ	bridging

ACKNOWLEDGEMENTS

I thank Professor Deryn Fogg for her incredible vision and commitment to teaching.

I am grateful to the Fogg group for assisting me in this learning process, especially Dr. Samantha Drouin and Professor Eduardo dos Santos for sharing their patience and expertise. Pawel, thanks for building a good friendship through this time with me, which I value greatly for the rest of our lives.

I am also very grateful to Professor Sandro Gambarotta for believing in my potential as a chemist, and Professor Darrin Richeson for his patience. Thanks Ilia, Jenn, Pat, and Davide and from the Gambarotta research group for your support.

Mom, Dad, and Omar, I love you so much for your unconditional support and love, I don't know if I can ever repay you guys.

PUBLICATION FROM THESIS WORK

- Amoroso, D.; Jabri, A.; dos Santos, E. N.; Gusev, D.; Yap, G. P. A.; Fogg, D. E.* "New Electron-Rich Ru-Pincer Complexes: Structure and Mechanism in Transfer Hydrogenation Catalysis", *Organometallics*, **2004**, *23*, 4047.

CHAPTER 1

Introduction

1.1. Homogeneous Catalysis.

Homogeneous ruthenium catalysts promote a wide range of transformations[1] useful in the fine chemicals industry. These successes in various catalytic transformations are partly due to new ligand designs, resulting in increased activity and selectivity in catalysis enough so as to make it more economically viable.[2-4] Basic phosphines and N-heterocyclic carbenes have been reported to have an activating effect on two important ruthenium catalyzed reactions in the fine chemicals industry, hydrogenation[5] and metathesis.[6] Our group and others have reported that the metal center can be switched between the two forms of catalysis by changing the active site from an alkylidene to a hydride, while retaining the same basic phosphine or NHC donors.[7-9] This has allowed for tandem catalysis applications for these two transformations, such that the ruthenium catalyst may be used in a more economical and convenient fashion.

Insights into the solution chemistry of a catalytic system from in situ observation have proven invaluable in homogeneous catalysis. In the context of hydrogenation chemistry, the work of Halpern[10] in the mechanism elucidation of rhodium catalyzed hydrogenation of olefins with bidentate phosphines has demonstrated the utility of increasing our understanding of a specific catalytic

system, as it provides a rational working hypothesis to understand and further improve a system.

1.2. Pincer Complexes.

Chelating ligands help define the active site of a metal center, thus allowing greater selectivity while also inhibiting deactivation processes.[11] The tremendous interest in organometallic complexes containing pincer ligands (Figure 1.1) (a recent search reveals 634 Chemical Abstracts entries for articles containing "pincer" in the title, including 57 entries for both "ruthenium" and "pincer" in the title) has been driven in large part by the potential of such species in catalysis.[12-17]

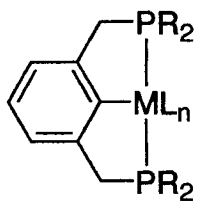

Figure 1.1. PCP pincer class of ligand on metal.

Pincer ligands are bound η^3 to a transition metal usually in a planar meridional fashion, in which the two neutral donors are located trans to each other and cis to a metal-carbon bond. This bonding motif is thought to stabilize metal complexes, and has been employed extensively in catalysis. Such complexes exhibit versatile catalytic activity in transfer hydrogenation, alkane

dehydrogenation, atom-transfer radical polymerization (ATRP), ring-opening metathesis polymerization (ROMP), and oxidative coupling of arenes with alkenes.[12-14,17-20]

Most of the PCP systems reported to date have used aryl-phosphine ligands.[12] Bulky alkyl-phosphine pincers could expand opportunities for tuning activity and selectivity of the metal center, and possibly even incorporating two consecutive mechanistically different tandem processes, such as olefin metathesis followed by transfer hydrogenation. A further more ambitious goal lies in the introduction of chirality into the pincer ligand to provide enantioselectivity for both processes.

1.3. Transfer Hydrogenation.

Transfer hydrogenation[21] is a very attractive form of catalysis to employ in a reduction when compared to direct hydrogenation, due to the convenient use of ordinary glassware instead of high-pressure bombs and flammable gasses. This is usually carried out in an alcohol solvent as the reducing agent, instead of using H_2 gas (Figure 1.2). The disadvantages of transfer hydrogenation with alcohols are that it requires a large excess of solvent relative to the substrate to drive the reaction to completion, since there is no strong thermodynamic driving force and it is a reversible, equilibrium process. Such a high substrate dilution can lower the rate of catalysis. The major advantage in direct hydrogenation over transfer

hydrogenation is that the reaction is highly exothermic and will therefore go to completion more readily, eliminating the need for excess solvent.

Figure 1.2. Transfer hydrogenation catalysis.

1.4. The Scope of This Thesis.

This thesis describes three main areas of investigation. Chapter 3 discusses the mechanistic investigation of known ruthenium pincer complexes in transfer hydrogenation, revealing new insights into the underlying transformations under catalytic conditions. Chapter 4 is describes the synthesis of new pincer ligands based on pyrrolide chelated to basic N-heterocyclic carbenes. Finally, Chapter 5 discusses the results of catalytic investigations of ruthenium complexes of secondary phosphines in transfer hydrogenation catalysis, and the underlying inorganic chemistry involved.

References

(1) Naota, T.; Takaya, H.; Murahashi, S.-I. *Chem. Rev.* **1998**, *98*, 2599.
(2) Chaloner, P. A.; Esteruelas, M. A.; Joo, F.; Oro, L. A. *Homogeneous Hydrogenation.* Kluwer: Boston, 1994.
(3) Noyori, R. *Asymmetric Catalysis in Organic Synthesis.* John Wiley & Sons: New York, 1994.
(4) Parshall, G. W.; Ittel, S. D. *Homogeneous Catalysis.* Wiley-Interscience: Toronto, 1992.
(5) Lee, H. M.; Smith, D. C.; He, Z.; Stevens, E. D.; Yi, C. S.; Nolan, S. P. *Organometallics* **2001**, *20*, 794.
(6) Fürstner, A. *Angew. Chem., Int. Ed.* **2000**, *39*, 3013.
(7) Sutton, A. E.; Seigal, B. A.; Finnegan, D. F.; Snapper, M. L. *J. Am. Chem. Soc.* **2002**, *124*, 13390.
(8) Louie, J.; Bielawski, C. W.; Grubbs, R. H. *J. Am. Chem. Soc.* **2001**, *123*, 11312.
(9) Drouin, S. D.; Zamanian, F.; Fogg, D. E. *Organometallics* **2001**, *20*, 5495.
(10) Halpern, J.; Riley, D. P.; Chan, A. S.; Pluth, J. J. *J. Am. Chem. Soc.* **1977**, *99*, 8055.
(11) Crabtree, R. H. *The Organometallic Chemistry of the Transition Metals.* Wiley-Interscience: Toronto, 1994.
(12) Albrecht, M.; van Koten, G. *Angew. Chem., Int. Ed.* **2001**, *40*, 3750.
(13) Albrecht, M.; Kocks, B. M.; Spek, A. L.; van Koten, G. *J. Organomet. Chem.* **2001**, *624*, 271.
(14) van der Boom, M. E.; Milstein, D. *Chem. Rev.* **2003**, *103*, 1759.
(15) Vigalok, A.; Milstein, D. *Acc. Chem. Res.* **2001**, *34*, 798.
(16) Jensen, C. M. *J. Chem. Soc., Chem. Commun.* **1999**, 2243.
(17) Milstein, D. *Pure Appl. Chem.* **2003**, *75*, 445.
(18) van de Kuil, L. A.; Grove, D. M.; Gossage, R. A.; Zwikker, J. W.; van Koten, G. *Organometallics* **1997**, *16*, 4985.
(19) Gossage, R. A.; van de Kuil, L. A.; van Koten, G. *Acc. Chem. Res.* **1998**, *31*, 423.
(20) del Rio, I.; van Koten, G. *Tetrahedron. Lett.* **1999**, *40*, 1401.
(21) Noyori, R.; Hashiguchi, S. *Acc. Chem. Res.* **1997**, *30*, 97, and references therein.

CHAPTER 2

Experimental Procedures

2.1. Materials and Methods.

2.1.1. Solvents.

Reagent grade toluene, hexanes, diethyl ether and tetrahydrofuran (BDH) were dried and degassed using an Anhydrous Engineering solvent purification system. Other solvents were refluxed over and distilled from an appropriate drying agent under an atmosphere of N_2: benzene over sodium benzophenone ketyl; pentane over sodium; dichloromethane, isopropanol, and pyridine over calcium hydride; methanol over Mg/I_2. All solvents (with the exception of methanol and isopropanol) were stored over Linde 4 Å molecular sieves under an atmosphere of N_2. Deuterated solvents ($CDCl_3$, C_6D_6, C_7D_8, THF-d_8, and D_2O) were obtained from Cambridge Isotope Laboratories Ltd. $CDCl_3$ was refluxed over and distilled from Drierite under an atmosphere of N_2. C_6D_6 was deoxygenated by consecutive freeze/pump/thaw cycles and stored over Linde 4 Å molecular sieves. All other deuterated solvents were used as received, in ampoule form.

2.1.2. Gases.

Hydrogen (Praxair UHP grade) and argon (Research Grade) were passed through a Drierite column before use.

2.1.3. Phosphines.

Phenylphosphine, diphenylphosphine, triphenylphosphine, and dicyclohexylphosphine (Strem) were used as received. All phosphines, with the exception of PPh_3, were stored under N_2.

2.1.4. Other Materials.

Benzophenone, potassium hydride, copper(I) chloride, HCl (2.0 M in Et_2O), and potassium tri(sec-butyl)borohydride (1.0 M in Et_2O) were purchased from Aldrich and used as received. Triethylamine (Aldrich) was distilled from $CaSO_4$ and stored under N_2. Hydrated $RuCl_3$ (38-43% Ru) and the Grubbs catalyst, $RuCl_2(PCy_3)_2(=CHPh)$ (**24**), were obtained from Strem Chemicals and used as received. $RuCl_2(PPh_3)_3$ (**1**),[1] $RuHCl(PPh_3)_3$ (**2**),[2] 1,3-$(Cy_2PCH_2)_2C_6H_4$ (dcpx),[3] $RuCl(\eta^3$-dcpx$)(PPh_3)$ (**7**),[4,5] $RuH(\eta^3$-dcpx$)(PPh_3)(N_2)$ (**8a/b**),[4,5] $RuH(\eta^3$-dcpx$)(PPh_3)(H_2)$ (**9a/b**),[4,5] $RuCl_2(HPCy_2)_4$ (**18a/b**),[6] $RuCl_2(HPPh_2)_4$ (**19a/b**),[6] $RuCl_2(H_2PPh)_4$ (**20a/b**),[6] and pyrrole ligand precursors[7] were prepared as previously described.

2.1.5. Instrumentation.

Infrared spectra were recorded on a Bomem MB100 IR spectrometer. Nuclear magnetic resonance (NMR) spectra were recorded on a Bruker Avance 300 (300 MHz for ^1H, 121 MHz for ^{31}P, 75 MHz for ^{13}C, 282 MHz for ^{19}F) or a Bruker AMX-500 (500 MHz for ^1H, 202 MHz for ^{31}P, 125 MHz for ^{13}C) FT-NMR

spectrometer. For ^{1}H and ^{13}C NMR spectra, the residual proton and carbon signals of the deuterated solvent were used as internal standards. ^{31}P NMR spectra were referenced externally against PPh_3 (δ_p –5.06, C_6D_6; -5.46, $CDCl_3$, -4.80, 2:1 isopropanol:C_7D_8): shifts are reported relative to 85% H_3PO_4. Downfield shifts are taken as positive for all nuclei. Variable temperature NMR spectra and 2D experiments (HMQC, HMBC, EXSY) were carried out on the Bruker Avance 300 or the Bruker AMX-500 instrument. Mass spectrometric analyses were performed by the Ottawa-Carleton Mass Spectrometry Centre. Gas chromatography data were obtained with an Agilent GC (6890N) instrument.

2.1.6. Laboratory Techniques.

Unless otherwise stated, all inorganic reactions containing ruthenium were carried out at room temperature (RT, ~22 °C) under N_2, using standard Schlenk or drybox techniques. Organic manipulations, other than those involving phosphine reagents, were carried out in air. All pyrrole compounds were stored cold (-19 °C) and protected from light.

2.2. Experimental Procedures for Chapter 3.

2.2.1. RuCl(η^3-dcpx)(PPh_3) (7): NMR-Scale.

(a) In the original report,[4] **7** was prepared by reaction of $RuCl_2(PPh_3)_3$ (**1**) with dcpx in toluene, in the presence of one equivalent of NEt_3. In this modification, no base was added. A mixture of $RuCl_2(PPh_3)_3$ (20 mg, 0.021 mmol)

and dcpx (10 mg, 0.021 mmol) in 1 mL toluene was stirred for 1 h, over which time it turned dark green. Quantitative conversion to **7** was confirmed by $^{31}P\{^{1}H\}$ NMR analysis.[4,5]

(b) In a further modification, $RuHCl(PPh_3)_3$ (**2**) was used as precursor in place of **1**. A mixture of **2** (20 mg, 0.022 mmol) and dcpx (10 mg, 0.022 mmol) in 1 mL C_6D_6 was stirred for 1 h. The solution turned dark green immediately. Quantitative conversion to **7** was confirmed by NMR analysis. $^{31}P\{^{1}H\}$ NMR (C_6D_6): δ 80.9 (t, Ru-*P*Ph_3, $^{2}J_{PP}$ = 32 Hz), 37.5 (d, Ru-*P*Cy_2, $^{2}J_{PP}$ = 32 Hz), –5.06 (s, *P*Ph_3).[4,5]

2.2.2. Conditions for in situ NMR experiment under catalytic conditions.

A solution of **7**•PPh_3 (7 mg, 0.006 mmol) in 0.3 mL C_7D_8 was mixed with a solution of KO^{t}Bu (13 mg, 0.012 mmol) in 0.6 mL isopropanol and heated at 82 °C under N_2. The solution was monitored by ^{31}P NMR spectroscopy over three days. Species present: (a) Before addition of base, RT: **7**. (b) 10 minutes after addition of base, RT: **8a/b**. (c) After 10 minutes pretreatment; spectrum at 80 °C: **6**. (d) After 1 h pretreatment; spectrum at RT: **8a/b** and **9a/b** (ratio of **8**:**9** = 99:1). (e) After 3 days at 80 °C; spectrum at RT: **9a/b**. $^{31}P\{^{1}H\}$ NMR (2:1 C_7D_8: isopropanol). For **7**: δ 81.2 (t, Ru-*P*Ph_3, $^{2}J_{PP}$ = 32 Hz), 37.0 (d, Ru-*P*Cy_2, $^{2}J_{PP}$ = 32 Hz). For **8a**: δ 60.5 (br, Ru-*P*Cy_2), 45.6 (t, Ru-*P*Ph_3, $^{2}J_{PP}$ = 17 Hz). For **8b**: 55.5 (br, Ru-*P*Cy_2) 29.4 (t, Ru-*P*Ph_3, $^{2}J_{PP}$ = 14 Hz). For **9a:** δ 68.9 (d, Ru-*P*Cy_2, $^{2}J_{PP}$ =

16 Hz), 57.0 (br, Ru-PPh$_3$). For **9b**: δ 71.8 (d, Ru-PCy$_2$, $^2J_{PP}$ = 15 Hz), 37.8 (br, Ru-PPh$_3$). For **10** (at 80 °C): δ 63-65 (br, Ru-PCy$_2$), 45.5 (br, Ru-PPh$_3$).

2.2.3. RuH(η^3-dcpx)(PPh$_3$) (10): NMR-scale.

A pale red solution of **8a/b** (10 mg, 0.01 mmol) in 1 mL C_6D_6 was frozen and placed under vacuum, then allowed to thaw under argon. The solution immediately turned deep red, and the spectrum was run within 10 minutes. ^{31}P NMR analysis showed **8b** and **10** (ratio 1:2). $^{31}P\{^1H\}$ NMR for **10** (C_6D_6): δ 63-65 (br, Ru-PCy$_2$), 45.3 (t, Ru-PPh$_3$, $^2J_{PP}$ = 17 Hz).

2.2.4. RuCl(η^3-dcpx)(PPh$_3$)(H$_2$) (11): NMR-Scale.

A dark green solution of **7**•PPh$_3$ (10 mg, 0.009 mmol) in 1 mL of C_6D_6 was placed under 1 atm of H_2 for 24 h. No colour change was observed, but ^{31}P NMR analysis (under H_2) revealed minor signals for **11** in addition to those for **7** (7% **11**). $^{31}P\{^1H\}$ for **11** (C_6D_6): δ 53.6 (d, PCy$_2$, $^2J_{PP}$ = 16.3 Hz), 23.2 (t, PPh$_3$, $^2J_{PP}$ = 16.3 Hz).

2.2.5. K[Ru(H)$_2$(η^3-dcpx)(PPh$_3$)] (13).

To a pale red solution of **8a/b** (25 mg, 0.028 mmol) in C_6D_6 (1 mL) was added KHB^{s}Bu$_3$ (28 μL of a 1.0 M solution in Et$_2$O, 0.028 mmol). The solution was stirred at 80 °C for 1 h, over which time a yellow suspension deposited. This was filtered off and dried under vacuum, leaving a colourless supernatant. Yield:

22 mg (90 %). Analysis of the latter showed no signal other than PPh_3. $^{31}P\{^1H\}$ NMR (protio-THF, unlocked): δ 74.6 (br, PCy_2), 67.3 (br, PPh_3).

2.2.6. Thermal Displacement of dcpx from 7 with PPh_3 and Base.

Solid **7**•PPh_3 (30 mg, 0.031 mmol) dissolved immediately upon addition to a solution of KO^{t}Bu (70 mg, 0.62 mmol) and PPh_3 (65 mg, 0.248 mmol) in 15 mL of isopropanol. A colour change to red occurred within minutes. The solution was heated at 80 °C for 1 h, which resulted in the precipitation of a yellow solid. This was filtered off and washed with 5 mL hexanes. ^1H NMR analysis reveals complete disappearance of the cyclohexyl signals for dcpx. Three different, unknown Ru-hydride species are present. ^1H NMR (C_6D_6): δ 7.5-6.5 (br, Ar*H*, 40 H), -8.52 (m, Ru*H*, 1 H), -10.23 (m, Ru*H*, 1H), -12.76 (br, Ru*H*, 1H). $^{31}P\{^1H\}$ NMR: δ 57.25 (d, PPh_3, $^2J_{PP}$ = 16 Hz, 4P), 50.15 (br, PPh_3, 1P), 44.67 (d, PPh_3, $^2J_{PP}$ = 16 Hz, 2P), 42.00 (br, PPh_3, 1P).

2.2.7. RuCl(η^3-dcpx)(py)$_2$ (14).

Solid **7** (100 mg, 0.087 mmol) was stirred in 2 mL of pyridine for 3 h, over which time the solution changed colour from green to bright orange. The solution was removed under vacuum to afford an orange oil. Addition of 5 mL of cold pentane precipitated a bright orange powder, which was then filtered and dried under vacuum. Yield 54 mg (80%). ^1H NMR (C_6D_6): δ 11.24 (m, py, *o*-C*H*, 2H), 7.92 (m, py, C*H*, 2H), 7.35 (d, dcpx *o*-CH, $^2J_{HH}$ = 7 Hz, 2H), 7.05 (t, dcpx *p*-C*H*,

$^2J_{HH}$ = 7 Hz, 1H), 6.55 (m, py, C*H*, 2H), 6.36 (m, py, C*H*, 2H), 5.87 (m, py, *o*-C*H*, 2H), 3.09 (s, PCH_2, 4H), 2.80 (br, Cy, 4H), 1.93-0.67 (br, Cy, 40H). $^{31}P\{^1H\}$ NMR: δ 42.36 (s, *P*Cy_2).

2.2.8. Representative procedure for transfer hydrogenation with 7•PPh_3.

A catalyst solution of standard concentration was prepared by dissolving **7**•PPh_3 (234 mg, 0.200 mmol) in 10.0 mL toluene. Likewise, a KOH solution of standard concentration was prepared by dissolving solid KOH (213 mg, 3.80 mmol) in 19.0 mL isopropanol, and a substrate solution of standard concentration by dissolving acetophenone (7.200 g, 0.060 mol) in 51 mL isopropanol. In a routine pretreatment procedure, 100 μL of the catalyst solution was mixed with 200 μL of the base solution, and the mixture was refluxed under N_2 for 1.0 hours. A colour change from dark green to red occurred within five minutes. After the pretreatment period, 1.70 mL (0.002 mmol) of the substrate solution was added by syringe. The reaction was monitored for 4 h, with sampling every ten minutes for the first hour, and every 30 minutes thereafter. Conversions were determined by gas chromatography.

2.2.8.1. Effect of Additives.

Transfer hydrogenations with **7**•PPh_3 were carried out as above, adding the freshly prepared catalyst solution to either one equivalent of CuCl (0.2 mg, 0.002 mmol), 8 equivalents of PPh_3 (4.2 mg, 0.016 mmol), or 20 equivalents of

N^nBu_4Cl (6.62 mg, 0.08 mmol). This was followed by pretreatment and addition of substrate solution as above.

2.3. Experimental Procedures for Chapter 4.

2.3.1. 2,5-Bis[(imidazolium)methyl]-pyrrole (15).

2-Iodopropane (2.04 g, 12 mmol) was added to 2,5-bis[(imidazol)methyl]-pyrrole[8] (1.00 g, 4.09 mmol) in 25 mL of DMF. The mixture was heated for 30 minutes at 70 °C, which resulted in complete conversion to **15** (confirmed by TLC). The solvent was then removed under reduced pressure, and the resulting brown solid was dissolved in 100 mL of distilled water, then filtered through Celite to remove insoluble purple byproducts, leaving a clear, colourless solution. This was added dropwise to a solution of NH_4PF_6 (1.36 g, 8.4 mmol) in 200 mL of dH_2O to yield a white precipitate, which was filtered off and washed with dH_20 (20 mL), then THF (2 x 20 mL). Yield after drying under vacuum 1.8 g (73%). ^1H NMR (DMSO-d_6) δ 11.32 (t, pyrr-N*H*, J_{HH}= 2.5 Hz, 1H), 9.15 (pseudo-t, imid-*H*1, J_{HH}= 2.5 Hz, 2H), 7.88 (pseudo-t, imid-*H*3, J_{HH}= 2.5 Hz, 2H), 7.65 (pseudo-t, imid-*H*4, J_{HH}= 2.5 Hz, 2H), 6.20 (d, pyrr-*H*3, J_{HH}= 2.5 Hz, 2H), 5.30 (s, CH_2, 4H), 4.63 (septet, $(CH_3)_2CH$, J_{HH}= 7 Hz, 2H), 1.45 (d, $(CH_3)_2CH$, J_{HH}= 7 Hz, 12H). $^{13}C\{^1H\}$ NMR: δ 135.3 (s, imid-*C*1), 126.5 (s, pyrr-*C*2), 123.1 (s, imid-*C*3), 121.5 (s, imid-*C*4), 110.5 (s, pyrr-*C*3), 53.2 (s, $(CH_3)_2CH$), 46.2 (s, CH_2), 23.1 (s, CH_3). IR (Nujol): ν(NH) 3389. ESI-MS: *m/z* Calcd for $C_{18}H_{27}F_6N_5P$ (M^+) 458; Found 458.

2.3.2. 2,5-Bis[(imidazolium)methyl]-pyrrole (16).

Methyl iodide (1.80 g, 13.0 mmol) was added to a solution of 2,5-bis[(imidazol)methyl]-pyrrole (1.00 g, 4.09 mmol) in 50 mL of THF. The solution was heated to reflux for 3 h, after which conversion to **16** was complete, as judged by TLC analysis. A white precipitate deposited, which was filtered off, washed with THF (2 x 20 mL), and dried under vacuum. Yield 1.9 g (85%). ^{1}H NMR (DMSO-d_6): δ 11.33 (t, pyrr-N*H*, J_{HH}= 2.5 Hz, 1H), 9.07 (pseudo-t, imid-*H*1, J_{HH}= 3 Hz, 2H), 7.71 (pseudo-t, imid-*H*4, J_{HH}= 3 Hz, 2H), 7.68 (pseudo-t, imid-*H*3, J_{HH}= 3 Hz, 2H), 6.20 (d, pyrr-*H*3, J_{HH}= 2.5 Hz, 2H), 5.34 (s, CH_2, 4H), 3.85 (s, CH_3, 6*H*). ^{13}C{^{1}H} NMR: δ 137.0 (s, imid-*C*1), 126.5 (s, pyrr-*C*2), 124.7 (s, imid-*C*3), 122.9 (s, imid-*C*4), 110.7 (s, pyrr-*C*3), 46.1 (s, *C*H$_2$), 36.9 (s, *C*H$_3$). IR (Nujol): ν(NH) 3391 cm^{-1}. ESI-MS: *m/z* Calcd for $C_{14}H_{21}N_5I$ (M^+) 384; Found 384.

2.3.3. 2-[(Imidazolium)methyl]-pyrrole (17).

2-Iodopropane (1.00 g, 6.00 mmol) was added to a solution of 2[(imidazol)methyl]-pyrrole (0.600 g, 4.00 mmol) in 25 mL DMF. Conversion was complete after heating to 70 °C for 15 min (TLC). The solvent was removed under reduced pressure to afford a brown solid. This was dissolved in 100 mL of distilled water, then filtered through Celite to remove insoluble purple byproducts. Dropwise addition of the filtrate to a solution of sodium tetraphenylborate (1.36 g, 8.4 mmol) in 200 mL dH_2O caused a white precipitate to deposit. This precipitate was filtered off and washed with 20 mL of d$H_2$0, then 2 x 20 mL of hexanes. Yield

1.5 g (83%). ^{1}H NMR (DMSO-d_6): δ 11.05 (m, pyrr-N*H*, 1H), 8.97 (pseudo-t, imid-*H*1, J_{HH}= 3 Hz, 1H), 7.17 (m, 7.64 (pseudo-t, imid-*H*5, J_{HH}= 3 Hz, 1H), 7.65 (pseudo-t, imid-*H*4, J_{HH}= 3 Hz, J_{HH}= 3 Hz, 1H), 6.20 (d, pyrr-H3, J_{HH}= 2.5 Hz, 2H), 5.30 (s, CH_2, 4H), 4.63 (septet, C*H*, J_{HH}= 7 Hz, 1H), 1.45 (d, C*H*3, *J*HH= 7 Hz, 6H). ^{13}C{^{1}H} NMR: δ 135.3 (s, imid), 126.5 (s, pyrr), 123.1 (s, imid), 121.5 (s, pyrr), 53.2 (s, *C*HMe$_2$), 46.2 (s, *C*H$_2$), 23.1 (s, *C*H$_3$). IR (Nujol): v(NH) 3407. ESI-MS: *m/z* Calcd for $C_{35}H_{36}BN_3$ (M^+) 411; Found 411.

2.4. Experimental Procedures for Chapter 5.

2.4.1. $RuCl_2(HPCy_2)_4$ (18a or 18b): NMR Scale.

(a) Cis isomer, **18a**: In the literature route,[6] a mixture of the cis and trans isomers (**18a** and **18b**, respectively) was obtained by thermolysis of $RuCl_3$ and $HPCy_2$ in methanol. In the present route, the cis isomer was selectively prepared by use of well-defined precursors. Thus, addition of $HPCy_2$ (13 mg, 0.065 mmol) to a brown suspension of $RuCl_2(PPh_3)_3$ (15 mg, 0.0156 mmol) in 1 mL C_6D_6 afforded a clear solution within minutes at room temperature. In situ ^{31}P{^{1}H} NMR analysis reveals the characteristic signals for **18a**.[6] ^{31}P{^{1}H} NMR (C_6D_6): δ 51.54 (t, $^2J_{PP}$ = 27 Hz), 24.39 (t, $^2J_{PP}$ = 27 Hz).

(b) Trans isomer, **18b**: In a second modification, **18b** was prepared by displacing the ligands from the Grubbs catalyst. Thus, $HPCy_2$ (22 mg, 0.1 mmol) was added to a purple solution of Grubbs catalyst (15 mg, 0.018 mmol) in 1 mL C_6D_6 at room temperature. Within 10 minutes, the solution turned clear yellow. In

situ NMR analysis reveals **18b**,[6] accompanied by singlets for free PCy_3 (11.03 ppm) and $P(CH_2Ph)Cy_2$ (3.10 ppm), as well as free (excess) $HPCy_2$ (-26.51 ppm). $^{31}P\{^1H\}$ NMR (C_6D_6) for **18b**: δ 14.56 (s).

2.4.2. $RuHCl(HPCy_2)_4$ (21).

$HPCy_2$ (60 mg, 0.3 mmol) was added to a purple suspension of $RuHCl(PPh_3)_3$ (30 mg, 0.06 mmol) in 1 mL of C_6D_6 to afford a clear, colourless solution within 15 minutes at room temperature. In situ $^{31}P\{^1H\}$ NMR analysis shows complete reaction. Addition of hexanes precipitated a microcrystalline white powder. Yield 53 mg (95%). ^1H NMR (C_6D_6): δ 4.46 (m, P*H*, 4H), 3.2-0.8 (br, Cy*H*, 88H), –19.92 (pentet, Ru*H*, $^2J_{PH}$ = 14 Hz, 1H). $^{31}P\{^1H\}$ NMR (C_6D_6): δ 35.66 (s, H*P*Cy_2).

2.4.3. $RuH_2(HPCy_2)_4$ (22).

To a yellow solution of $RuCl_2(HPCy_2)_4$ **18a/b** (30 mg, 0.03 mmol) in THF was added KHB^sBu_3 (64 uL of 1M solution in diethyl ether, 0.064 mmol) at room temperature. The solution decolourized within minutes, and in situ $^{31}P\{^1H\}$ NMR analysis shows complete reaction. Addition of hexanes precipitated a microcrystalline white powder. Yield 25 mg (80%). $^{31}P\{^1H\}$ NMR (protio-THF, unlocked): δ 50.70 (t, H*P*Cy_2, $^2J_{PP}$ = 22 Hz), 38.80 (t, H*P*Cy_2, $^2J_{PP}$ = 22 Hz).

2.4.4. RuCl(η^3-dcpx)(H_2PPh)$_2$ (23).

H_2PPh (40 mg, 0.36 mmol) was added to a dark green solution of RuCl(η^3-dcpx)(PPh_3) **3** (200 mg, 0.17 mmol) in 3 mL toluene. The solution turned clear yellow within few minutes at room temperature. In situ $^{31}P\{^1H\}$ NMR analysis shows solely the A_2BC splitting pattern due to **23**. Addition of hexanes precipitated a microcrystalline yellow powder. Yield 210 mg (92%). $^{31}P\{^1H\}$ NMR (C_7H_8, unlocked): δ 52.25 (dd, PCy_2, $^2J_{PP}$ = 34 Hz, $^2J_{PP}$ = 20), -15.55 (dt, H_2PPh, $^2J_{PP}$ = 34 Hz, $^2J_{PP}$ = 19 Hz), -45.23 (td, H_2PPh, $^2J_{PP}$ = 19 Hz, $^2J_{PP}$ = 20 Hz).

References

(1). Hallman, P. S.; Stephenson, T. A.; Wilkinson, G. *Inorg. Synth.* **1970**, *12*, 237.

(2). Amoroso, D.; Snelgrove, J. L.; Conrad, J. C.; Drouin, S. D.; Yap, G. P. A.; Fogg, D. E. *Adv. Synth. Catal.* **2002**, *344*, 757.

(3). Gusev, D. G.; Madott, M.; Dolgushin, F. M.; Lyssenko, K. A.; Antipin, M. Y. *Organometallics* **2000**, *19*, 1734.

(4). Amoroso, D. Ph. D. Thesis, University of Ottawa, 2002.

(5). Amoroso, D.; Jabri, A.; Yap, G. P. A.; Gusev, D. G.; dos Santos, E. N.; Fogg, D. E. *Organometallics* **2004**, *23*, 4047.

(6). Simpson, R. H. *J. Chem. Soc. Dalton Trans* **1994**, 3377.

(7). Kim, I. T.; Elsenbaumer, R. L. *Tet. Lett.* **1998**, *39*, 1087.

(8). Kim, I. T.; Elsenbaumer, R. L. *Chem. Commun.* **1998**, 327.

CHAPTER 3

Mechanistic Insights Into Transfer Hydrogenation involving a Ruthenium-Pincer Ligand Complex

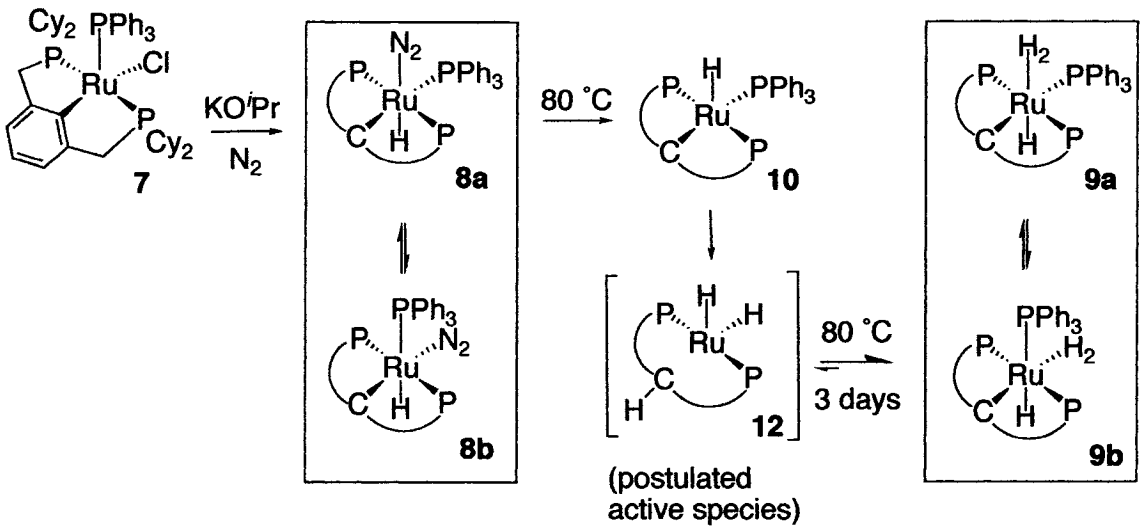

Figure 3.1. Pictorial summary of Chapter 3.

Part of this Chapter has been published:
Amoroso, D.; Jabri, A.; dos Santos, E. N.; Gusev, D.; Yap, G. P. A.; Fogg, D. E.* "New Electron-Rich Ru-Pincer Complexes: Structure and Mechanism in Transfer Hydrogenation Catalysis", *Organometallics*, **2004**, *23*, 4047.

3.1. Introduction.

The general importance of transition metal-catalyzed transfer hydrogenation was discussed in Chapter 1. Of particular interest is the effect of base. For example, the rate of hydrogen transfer from secondary alcohols to ketones in the presence of transition metal complexes such as $RuCl_2(PPh_3)_3$ (**1**) is enhanced if a small quantity of KOH is added to the system.[1] In a seminal contribution, Bäckvall and co-workers reported that the monohydride species $RuHCl(PPh_3)_3$ (**2**) is initially formed on heating **1** in basic isopropanol, but that this is then converted into the dihydride species $RuH_2(PPh_3)_3$ (**3**).[2] They identified **3** as the catalytically active species in transfer hydrogenation of acetophenone, as **3** was able to effect reduction in the absence of added base. The hydrogenation most likely occurs by a conventional, inner-sphere mechanism, which requires coordinative unsaturation for high activity (Figure 3.2).

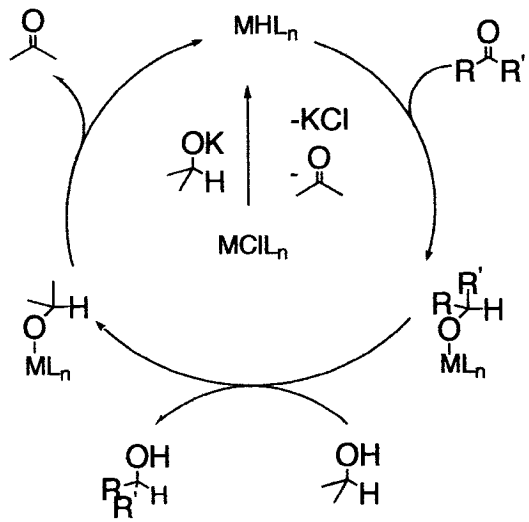

Figure 3.2. A generic catalytic cycle for transfer hydrogenation via an inner-sphere mechanism.

Research by van Koten and coworkers has shown that Ru(II) complexes of the dppx pincer ligand, $RuX(\eta^3\text{-dppx})(PPh_3)$ (Figure 3.3; dppx = 1,3-bis[(diphenylphosphanyl)-methyl]-benzene), have high activity in transfer hydrogenation of ketones. For example, in hydrogenation of acetophenone, complex **4a** achieved a good turnover frequency (TOF = (mol substrate converted)(mol catalyst)$^{-1}h^{-1}$ of 2,300 h^{-1} at 50% conversion (in comparison to the poor TOF of 100 h^{-1} for the reduction of the more challenging substrate, benzophenone under the same conditions). Base was required for this transformation; the ratio of base to catalyst was 20:1, which is the standard ratio used.[3-5] Higher activity was found for **4b**, which contains a weakly bound triflate ligand. In comparison, Samantha Drouin of this research group reported extremely high turnover frequencies (9,600 h^{-1} at 50% conversion) for transfer hydrogenation of benzophenone using $RuH(CO)[(OC(Ph)(C_6H_4)]$(dcypb) (**6**) (dcypb = 1,4-bis(dicyclohexyl)phosphinobutane).[6,7] No data were collected for acetophenone reduction. The highly active "Noyori-class" catalyst $RuCl_2$(dppe)(en), which utilizes an outer-sphere mechanism, achieves a TOF of 6,700 at 50% conversion for reduction of acetophenone under conditions similar to those used for **4a**.[8]

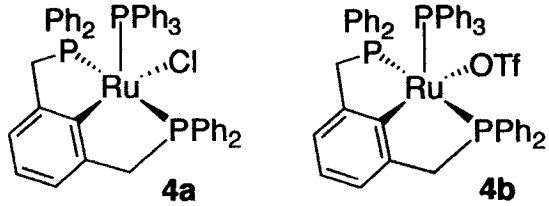

Figure 3.3. Ruthenium complexes containing an arylphosphine "PCP-pincer" ligand, **4a** and **4b**.

Transfer hydrogenations involving **4a/b** were carried out in the presence of base and isopropanol, conditions which were proposed to effect formation of the anionic mono-hydride species, $[RuH(O^iPr)(\eta^3\text{-PCP})(PPh_3)]^-$ (**5**).[5] Notable in **5** is retention of the η^3-PCP "pincer" ligand, the stability of which is often cited as an advantage of such ligands in catalysis, in that it contributes to greater catalyst robustness.[9] The stability of the ligand architecture is also viewed as critical to asymmetric catalysis via chiral pincer ligands. In contrast to the Noyori catalyst $RuCl_2$(binap)(en*),[8] (en* = a chiral diamine) however, chiral Ru-pincer complexes have not yet enabled high enantioselectivities in transfer hydrogenation.[9]

While Group 9 and 10 metal complexes with aryl- and alkyl-PCP ligands have received much attention, the PCP-pincer chemistry of Group 8 metals has focused principally on the important family of arylphosphine derivatives, as indeed exemplified by **4a**. Examples of alkylphosphine-pincer complexes in Group 8 chemistry are confined to tert-butyl[10-13] and isopropyl[14] PCP ligands, but these have not been explored in catalysis. In view of the profound influence of pincer ligand properties and chelate bite angles on structure and reactivity,[9] and motivated by the high transfer-hydrogenation activity of the cyclohexylphosphine complex **6** noted above,[6,7] our group was interested in the possibility of improving

the activity of the Ru-pincer systems by incorporating cyclohexylphosphine donors. Group 9 and 10 complexes of the dcpx ligand (dcpx = 1,3-bis[(dicyclohexylphosphanyl)-methyl]-benzene) have been studied by the Cross[15-18] and Park[19-22] groups, but this ligand was not used in ruthenium chemistry prior to our efforts.

With the intention of examining the effect of increased ligand basicity on catalyst activity in transfer hydrogenation, Dr. Dino Amoroso of this research group synthesized and characterized the dcpx complex analogue of **4a**. Thus, high-yield routes were established to RuCl(η^3-dcpx)(PPh_3) (**7**), as well as its hydride derivatives RuH(η^3-dcpx)(PPh_3)(N_2) (**8a/b**) and RuH(η^3-dcpx)(PPh_3)(H_2) (**9a/b**), Figure 3.4.[23,24] These complexes are close structural analogues to the earlier-reported phenyl, isopropyl, and tert-butyl PCP-pincer complexes.[14-16,25] Preliminary catalytic studies of **7** and **8a/b** were carried out.[23,24] In the present work, a detailed mechanistic investigation was undertaken. A key, unexpected finding in this work is indirect evidence for an active catalyst containing an η^2-bound pincer ligand, which may limit catalyst lifetime and/or selectivity.

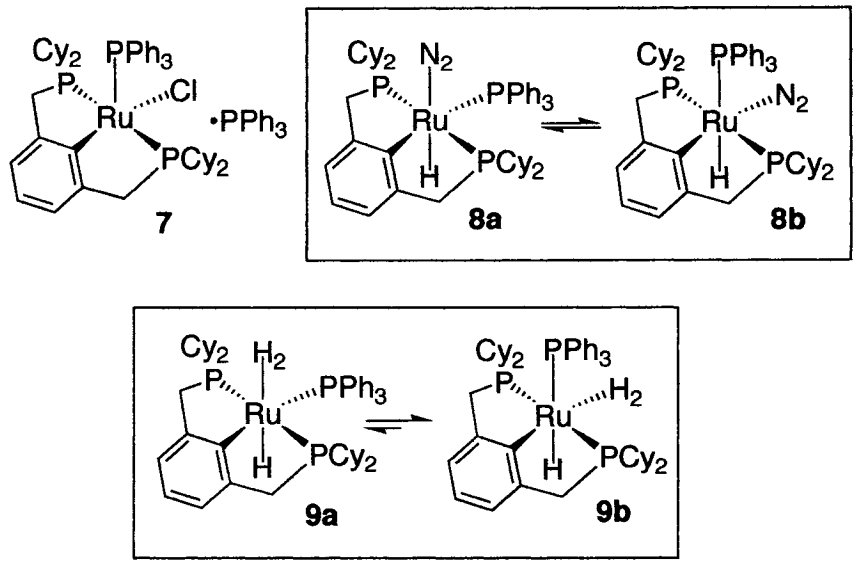

Figure 3.4. Cyclohexylphosphine pincer complexes **7**, **8a/b** and **9a/b**.

3.2. Synthesis of RuCl(η^3-dcpx)(PPh_3) (7).

In our original synthesis of **7**·PPh_3, $RuCl_2(PPh_3)_3$ (**1**) was reacted with one equivalent of dcpx in the presence of NEt_3. The product was isolated as the PPh_3 solvate. In keeping with suggestions from other groups, we initially assumed that the reaction proceeded via deprotonation of the $RuCl_2(\eta^2$-PC(H)P-arene)(PPh_3) intermediate by NEt_3.[11,26-28] In the present work, however, reaction of $RuCl_2(PPh_3)_3$ (**1**) with dcpx was found to effect complete formation of **7** at room temperature, even in the absence of NEt_3 (Figure 3.5a). This implies that the $RuCl_2(\eta^2$-PC(H)P-arene) intermediate is sufficiently acidic to be deprotonated by PPh_3. The pK_a of PPh_3·HCl is 2.73, as compared to 10.75 for NEt_3·HCl.[29]

In an alternative synthetic route, **7** was prepared by reaction of $RuHCl(PPh_3)_3$ (**2**) with dcpx. The stoichiometry of the reaction requires loss of H_2, and indeed evolution of gas is noted in the reaction (Figure 3.4b). This reactivity

suggests that formation of **7** with loss of H_2 gas is energetically favored over an η^2-bound RuHCl(η^2-PC(H)P-arene) intermediate.

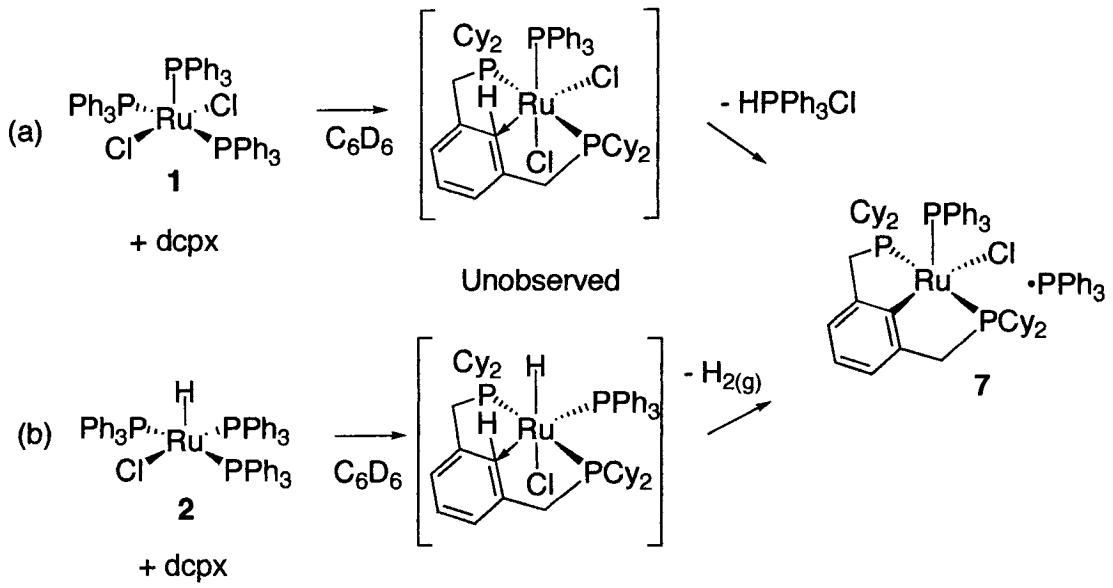

Figure 3.5. Synthesis of **7** from (a) $RuCl_2PPh_3$ (**1**) or (b) $RuHCl(PPh_3)_3$ (**2**) without added base.

3.3. Transfer hydrogenation by RuCl(η^3-dcpx)(PPh_3) (7).

Previous work by Dino Amoroso demonstrated that **7**•PPh_3 was an effective catalyst for hydrogenation of benzophenone in the presence of base co-catalyst. As noted above, however, reduction of benzophenone is more challenging than reduction of acetophenone. With the intention of expanding our mechanistic understanding of this reaction using an experimentally convenient substrate, we undertook a detailed study of the transfer hydrogenation of acetophenone. Reactions were monitored by gas chromatography. Turnover

frequencies (TOF) were cited at 20% conversion, in order to minimize the influence on the rate of decreases in substrate concentration (Table 3.1).

Table 3.1. Transfer hydrogenation of acetophenone using precatalyst **7**•PPh_3.[a]

Entry	Pretreatment time [b] (min)	Additive	TOF [c] (h^{-1})
1	0	KOH	300
2	10	KOH	450
3	60	KOH	1300
4	60	KO^{t}Bu	1300
5	60	KOH + N^{n}Bu$_4$Cl [d]	320
6	60	KOH + PPh_3 [e]	480
7[f]	60	KO^{t}Bu / H_2	2500

[a] Conditions: 2.0 mmol acetophenone, [Ru] = 0.1 mol %, additives 2.0 mol %, 2.0 mL ^{i}PrOH, reflux (82 °C), N_2 atmosphere, unless otherwise noted. [b] Precatalyst heated in presence of base before addition of substrate. [c] Mol substrate converted per mol Ru per *h* at 20% conversion [d] 2 mol % N^{n}Bu$_4$Cl. [e] 0.8 mol % PPh_3, [f] Reaction and pretreatment under H_2 (1 atm).

At high concentrations, strong base (including alkali metal hydroxides) can effect hydrogen transfer of isopropanol to ketones, via a process related to the classical Meerwin-Ponndorf-Verley (MPV)[30] reduction using aluminum alkoxides.[31-33] While forcing conditions are typical (temperatures up to 150 °C),

rates can be significant even at 82 °C. LePage and James, for example, report 60% conversion of acetophenone to 1-phenylethanol within 4 h, for reactions in refluxing isopropanol with 34 mol % NaOH, relative to substrate.[34] While this might suggest that base catalysis is preferable to transition-metal catalysis, the disadvantages of high base concentrations (such as the self-condensation of enolizable ketone-containing substrates)[29] limits the usefulness of MPV catalysis to non-enolizable ketones such as benzophenone.

In some cases, MPV chemistry may go unrecognized.[35-37] For example, Le Floch and coworkers recently reported extraordinary activity (TON >18 x 10^6) for transfer hydrogenation of acetophenone by RuCl(η^6-p-cymene)((1,2-methylpyridine)phosphole).[38] While the "catalyst" concentration was extremely low (5 x 10^{-6} mol % Ru relative to acetophenone), the base concentration was 34 mol %. A parallel with the base-catalyzed reaction conditions reported by LePage and James is obvious: the true TON, assuming that NaOH is the catalyst, is a more realistic value of 2.

In order to rule out the possibility that MPV chemistry contributes to the reduction of acetophenone under our standard conditions (2 mol % KOH, 82 °C), we carried out a control experiment involving incubation of substrate with base in the absence of the ruthenium catalyst **7**. This results in only 2% reduction of acetophenone after 4 h, indicating that MPV reduction does not contribute significantly.[39] Catalyst activity is very sensitive to the *duration* of pretreatment (heating of the precatalyst in basic isopropanol before addition of the substrate).

After only 10 minutes of pretreatment, the activity increases by 50% relative to the reactions carried out in the absence of this initial heating step. The activity increases four-fold after 1 h of pretreatment (Entries 1-3). Approximately identical activity was found using KOH or KO^{t}Bu, although the base strength varies by three orders of magnitude (pK_a KOH = 16; pK_a KO^{t}Bu = 19; Entries 3, 4). This suggests that the base is not involved in the rate-determining step, but rather promotes formation of the catalytically active species, most probably in a rapid pre-equilibrium involving formation of the isopropoxide ion.[40,41] More than 1 h of pretreatment did not measurably enhance the catalysis any further, which suggests after the 1 h pretreatment, no more catalytically active species forms.

Finally, we note that under a hydrogen atmosphere the catalyst activity at 20% conversion (Entry 7) is double than that observed under a nitrogen atmosphere (as found previously[23,24] for benzophenone reduction). This higher activity may imply that both direct H_2 hydrogenation and transfer-hydrogenation pathways are involved. Alternatively, coordination of N_2 may be responsible. Dino Amoroso earlier described the efficacy of N_2 in binding to other Ru-dicyclohexylphosphine complexes.[42]

Addition of the soluble chloride donor N^{n}Bu$_4$Cl (20 equiv per Ru) reduces the activity of the catalyst to the level observed without pretreatment (Entries 1, 5). Excess chloride is presumed to compete with the substrate for coordination to the metal center. Its inhibiting effect is consistent with van Koten's report that complex **4b**, containing the weakly coordinating triflate ion, is much more active

than its chloride analogue **4a**.[5] Addition of PPh_3 to the system also diminishes the activity; this suggests that an equilibrium involving loss of PPh_3 precedes the rate-determining step, and that excess PPh_3 can compete with the substrate for vacant sites. Both the bound and the solvating PPh_3 present in the precatalyst **7**•PPh_3 will thus diminish the overall activity of the system. Attempts to generate a more active catalytic species by addition of CuCl as a phosphine scavenger also resulted in decreased activity.[43] This suggests that unwanted deactivating interactions of the CuCl with the ruthenium catalyst occurs.

3.4. In situ NMR experiments under catalytic conditions.

In view of the marked dependence of catalytic activity on pretreatment time, in situ NMR analysis of the precatalyst **7** under the conditions of catalysis was undertaken in order to gain insight into the nature of the active species (Figure 3.6). In these experiments, KO^tBu was used in preference to KOH, in order to ensure that the base dissolves fully.

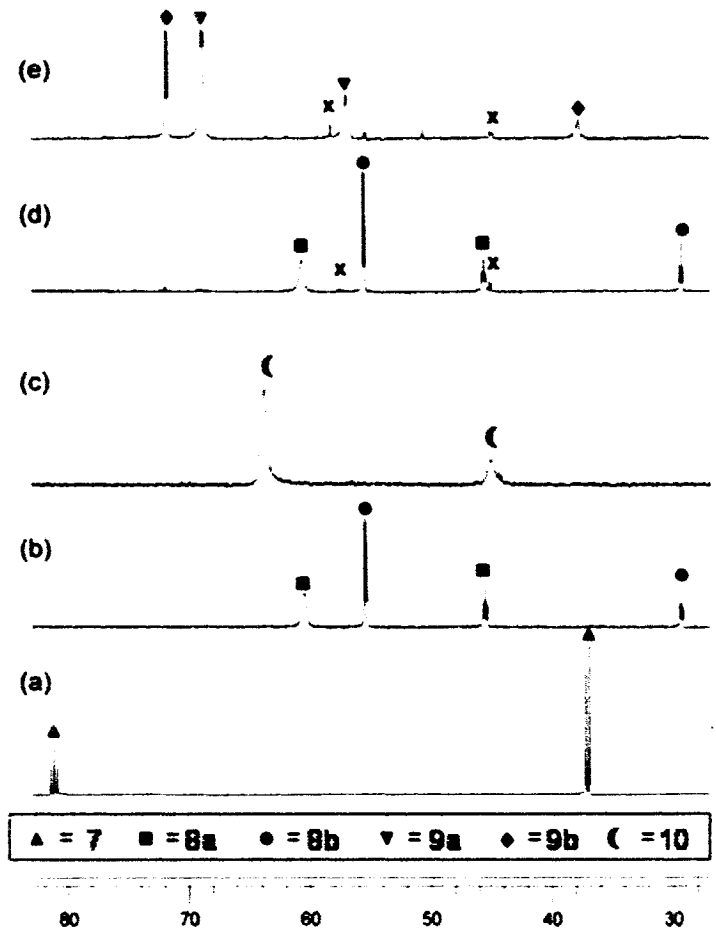

Figure 3.6. In situ $^{31}P\{^1H\}$ NMR spectra of precursor **7** under transfer hydrogenation conditions (2:1 isopropanol: C_7D_8, N_2 atmosphere, 20 equiv KO^{t}Bu). (a) Before addition of base; 22 °C. (b) 10 min after adding base; 22 °C. (c) After 10 minutes at 80 °C (spectrum measured at 80 °C). (d) After 1 h at 80 °C (spectrum measured at 22 °C). (e) After 3 days at 80 °C (spectrum measured at 22 °C).

After 10 minutes in the presence of base and isopropanol at *ambient temperature* under N_2, the signals for **7** (Figure 3.6a) have disappeared completely, being replaced by two new A_2B patterns assigned to **8a/b** (Figure 3.6b and Table 5.2; ratio 1:1). The latter assignments were confirmed by $^{31}P\{^1H\}$ NMR analysis of authentic samples of **8a/b** in 2:1 isopropanol: C_7D_8.

Table 5.2. Summary of $^{31}P\{^1H\}$ NMR data for complexes **7-10** under catalytic conditions.[a]

Cpd	$\delta_{P(A)}$ PCP	$\delta_{P(B)}$ PPh_3	$^2J_{PP}$
$RuCl(\eta^3\text{-dcpx})(PPh_3)$ (**7**)	37.0	81.2	31
$RuH(\eta^3\text{-dcpx})(PPh_3)(N_2)$ (**8a**)[b]	60.5	45.6	17
(**8b**)	55.5	29.4	14
$RuH(\eta^3\text{-dcpx})(PPh_3)$ (**10**)[c]	63-65	45.5 (br)	
[d]	63-65	45.3	17
$RuH(\eta^3\text{-dcpx})(PPh_3)(H_2)$ (**9a**)	68.9	57.0 (br s)	16
(**9b**)	71.8	37.8 (br s)	15

[a] 300 MHz (^{1}H); 121 MHz (^{31}P); 295K, *J* in Hz. All spectra recorded in 2:1 ^{i}PrOH: C_7D_8, unless otherwise noted. All PCP signals doublets; all PPh_3 signals triplets, unless otherwise noted. [b] Spectra at 253K; unresolved at 295K. [c] Spectra at 295K under N_2. [d] Spectra at 355K under Ar in C_6D_6.

Although N_2 remains bound to **8a/b** at room temperature, on warming the NMR probe, the signals due to dinitrogen-bound **8a** and **8b** progressively diminish until, at 82 °C, they disappear (Figure 3.6c and Table 3.2). The new spectrum is attributed to coordinatively unsaturated **10** (^{31}P, br 63-65 and 45 ppm; Table 3.2). The assignment of **10** was supported by exchanging the N_2 atmosphere of an NMR sample of **8a/b** with Ar at room temperature, instantly generating **10**. This result suggests that in electron-rich pincer complex **8a/b**, the bound dinitrogen can be thermally removed.

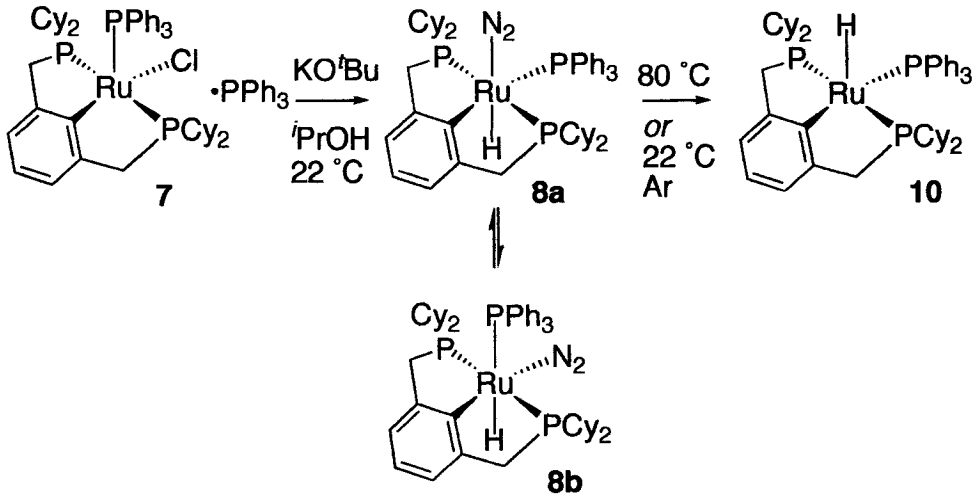

Figure 3.7. Synthesis of dinitrogen-bound monohydrides **8a/b** and dinitrogen-free monohydride **10**.

After the typical pretreatment period used in catalysis of 1 h at 82 °C, the spectrum is essentially unchanged: resonances for **10** still dominate the spectrum, accompanied by a new A_2B pattern (**X**; 1% integrated intensity) at δ 57.3(triplet), and 45.0 (doublet, $^2J_{PP}$ = 23 Hz), and emerging signals corresponding to RuH(η^3-dcpx)(PPh_3)(H_2) **(9a/b)** (<1% by $^{31}P\{^1H\}$ analysis, Figure 3.6c). The complexes **9a/b** exist as a mixture of two conformational isomers, with the hydride trans (**9a**) or cis (**9b**) to dihydrogen: the cis isomer predominates by a ratio of 3:1. The high stability of hydride cis to H_2 has been noted,[44] and may provide a driving force for exchange in the case of **8a/b**. The T_1(min) relaxation times for the dihydrogen ligand in **9a/b** were measured and found to be longer in **9b** than in **9a**, as expected for a dihydrogen ligand perturbed by a favorable interaction with a cis-hydride[44] (**9a**: 20 msec; **9b**, 24 msec; both at 265K, 500 MHz).

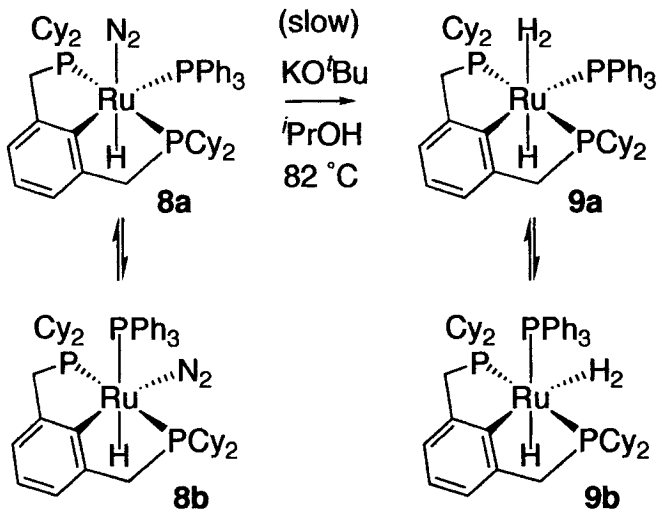

Figure 3.8. Formation of **9a/b** by thermolysis of **8a/b** in basic isopropanol. H_2 in **9a** is postulated to form from a dihydride intermediate as discussed below.

Our group reported previously that **8a/b** react readily with H_2 to form **9a/b,**[23,24] but the analogous reaction with chloride complex **7** gave only 7% by integration of a new A_2B system in the ^{31}P NMR spectrum (53.6 (d), 23.2 (t), $^2J_{PP}$ = 16.3 Hz) under 1 atm H_2 for 24 h. The multiplicity indicates retention of PPh_3 and the pincer ligand within the coordination sphere, and the structure is tentatively assigned as RuCl(η^3-dcpx)(PPh_3)(H_2) **11**.

As the probe is cooled back to room temperature after the 1 h pretreatment, the signals for **8a** and **8b** reappear (Figure 3.6c) and a 1:1 integration is re-established, but the new signals (**X**) and the signals for **8a/b** still remain as well. Further heating of the NMR sample for three days at 82 °C resulted in a colour change from red to pale yellow, with the ^{31}P NMR spectrum revealing clean conversion to the hydride complexes **9a** and **9b** (>98% by

integration). These results from the in situ NMR spectrum shown in Figure 3.6, when combined with the kinetic data discussed above (Table 3.1), give mechanistic insights into pincer complexes **7**, **8a/b**, **9a/b** and **10** in transfer hydrogenation catalysis.

In situ NMR analysis reveals no N_2-bound Ru species at the higher temperatures used in catalytic conditions. From the kinetic data, maximum activity requires a "pretreatment" period as long as 1 h, which was at first assumed to be necessary to convert all the ruthenium bulk species into the active species. However, the in situ NMR experiments surprisingly show complete conversion of **7** to monohydrides **8a/b** in <10 minutes even at room temperature, and no further spectroscopically observable change was observed after the 1 h pretreatment, despite a large change in activity. Thus, the monohydride complexes **8a/b** are probably not the catalytically most active species, but merely a resting state that delivers this species. Furthermore, the emergence of dihydrogen-bound monohydride species **9a/b** under nitrogen atmosphere strongly suggests the intermediacy in the catalysis of a dihydride species, and our observations provide strong circumstantial support for the accessibility of such an entity. The complexes **9a/b** are also concluded to be resting states, since we only observe a small rate increase when the reaction is run under H_2, whereas we would expect a very large increase in activity due to facile formation of **9a/b** under H_2. The absence of spectroscopic evidence for either a PPh_3-free or a dihydride species after the 1 h of pretreatment points towards the operation

of a highly active catalyst present in low concentration. A favored candidate is $Ru(H)_2[\eta^2$-PC(H)P](L) (**12**, L = solvent or substrate), formed by elimination of the activated pincer carbon. In favor of **12** are its coordinative unsaturation and enhanced flexibility.[45-47] One other possible candidate is anionic $K[Ru(H)_2(\eta^3$-dcpx)$(PPh_3)]$ **13**. This species would be less likely to be catalytically active due to its coordinative saturation. Attempted synthesis of **12** was unsuccessful due to the instability of this entity with respect to **9a/b**, the thermodynamic resting state of our system. To access **13**, one equivalent of KHB^sBu_3 was added to monohydride **8a/b** in benzene at 80 °C. A yellow solid precipitated out of solution within minutes (Figure 3.9). This yellow precipitate is only soluble in polar solvents such as THF, and appears to be fluxional in solution with two broad peaks in the ^{31}P NMR spectrum (74.6 and 67.3 in a 2:1 ratio). Initial catalytic trials show no catalytic activity for **13** under the standard transfer hydrogenation conditions. This result suggests that dihydride **13** is not the catalytically active species.

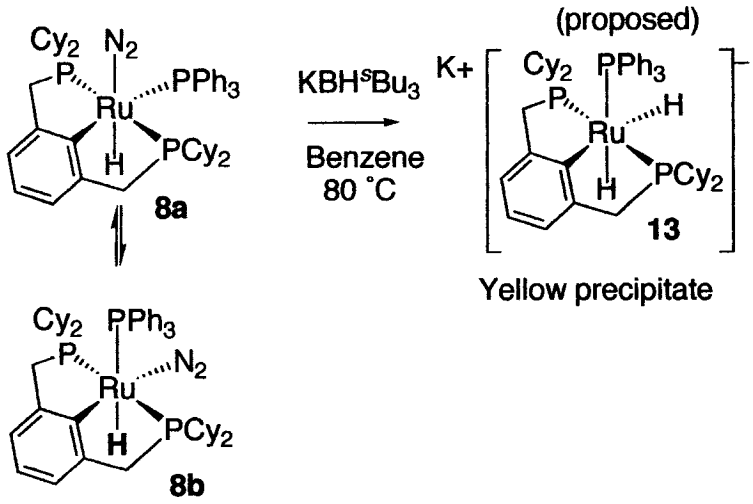

Figure 3.9. Synthesis of **13**.

Based on indirect evidence of dihydride formation and the evidence that a η^3-bound dihydride **13** is not the catalytically active species, we can postulate a transient η^2-bound PC(H)P Ru dihydride **12** as the active species (Figure 3.10). Since the activity under an H_2 atmosphere is approximately twice than that seen under a N_2 atmosphere, the barrier to formation of the active species is possibly lower when the catalysis is performed under the H_2 atmosphere.

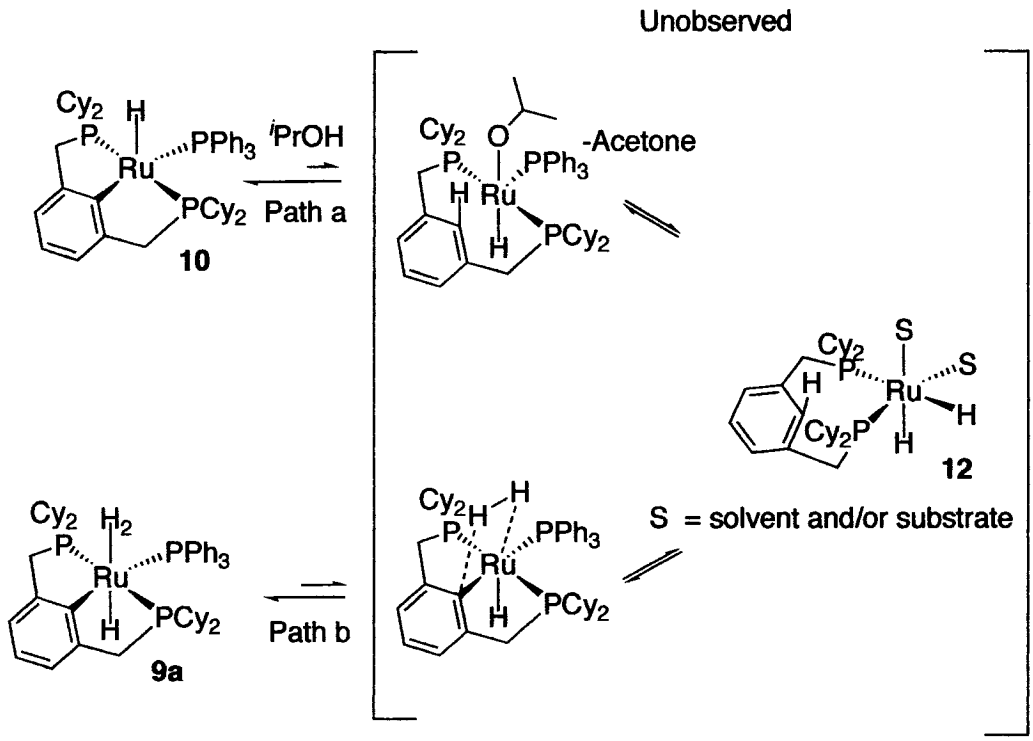

Figure 3.10. Two pathways leading to the proposed active catalyst, **12**.

One way that the dihydrogen-bound monohydrides **9a/b** could give rise to **12** more easily than the non-dihydrogen coordinated complex **8a/b** is through the lower energy route (compare path a and b, Figure 3.10) to **12** via heterolytic cleavage of H_2. This is the reverse of the process shown in Figure 3.4, where the synthesis of **7** results from the loss of an H_2 molecule from $RuHCl(PPh_3)_3$ and dcpx. Thus, even though the ruthenium-carbon bond is stable in catalytically inactive PCP pincer complexes in transfer hydrogenation, these results show that the ruthenium-carbon bond is possibly cleaved to form a catalytically active transient η^2-dcpx-bound **12**.

In addition, the ease with which the η^3-dcpx structure could be regenerated would give access to a stable resting state, accounting for the

thermal stability and robustness of the catalyst (supported by the observation that no decomposition occurs even after 3 days at 82 °C), as well as the spectroscopic invisibility of the η^2-species. However, an η^2-bound dcpx ligand in **12** would be more labile, suggesting it could be possible to displace the dcpx ligand in the presence of excess PPh_3. Addition of 8 equivalents of PPh_3 to a solution of **7**·PPh_3 in basic isopropanol, followed by heating results in the rapid precipitation of a yellow solid. ^1H NMR analysis of the solid shows only aryl peaks, with the absence of aliphatic peaks representative of the cyclohexyl groups on dcpx (Figure 3.11). This results suggests under catalytic conditions the dcpx ligand can be displaced from the metal center by PPh_3.

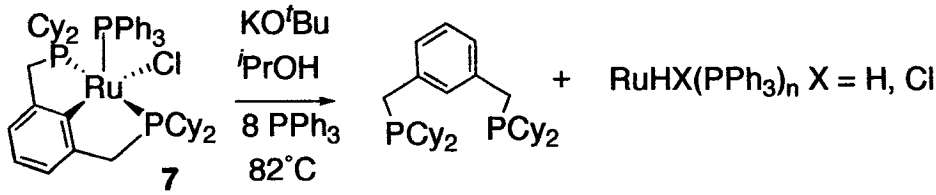

Figure 3.11. Loss of dcpx ligand under pretreatment conditions with added PPh_3.

The proposed active species **12** bears a resemblance to the highly active transfer hydrogenation catalyst synthesized by our group- cyclohexylphosphine complex K[RuH_3(dcypb)(CO)] **6**,[7] in that they both contain a bidentate dicyclohexyl phosphine ligand with a flexible backbone (Figure 3.12). The activity of **6** is higher by several orders of magnitude (TOF 9,600 h^{-1} for reduction of benzophenone) than precatalyst **7**, possibly due to the flexible backbone.

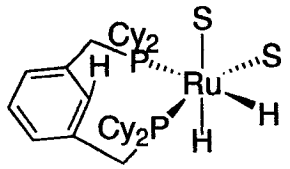

12

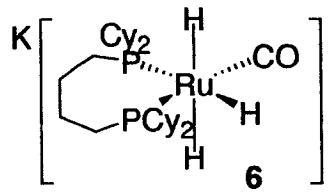

6

Figure 3.12. Proposed active species **12,** which is similar to highly active literature species, K[RuH_3(dcypb)(CO)] **6**.

One reproducible observation during the course of this work is that aged catalyst solutions (those dissolved in toluene in a Schlenk tube outside of the glove box for more than one week) were clearly more active in transfer hydrogenation catalysis than fresh catalyst solutions, with the absence of pretreatment steps in both cases (TOF at 50% conversion was 400 and 200 for the aged and fresh catalyst solution, respectively). Also, while freshly made catalyst solutions increased activity with pretreatment, the aged solutions showed no such enhancement. ^{31}P NMR analysis of a month old aged solution of catalyst shows 12 % by integration of new peaks at δ 52.5, 45.0, and 25.21 ppm that could be attributed to phosphine oxide formation. The recent review by Grushin[48] suggests that the formation of coordinatively unsaturated transition metal species via the oxidation of one bound phosphine (in chelating diphosphine systems) to a weakly bound hemi-labile phosphine-phosphine oxide chelate is common in catalysis. In other homogeneous systems in the literature,[49] aged batches of catalyst behave very differently than freshly made ones - sometimes completely switching the product selectivity - and this difference has been suggested to occur by in situ phosphine oxidation. If phosphine oxidation can create a

coordinatively unsaturated active species, then it could potentially activate precatalyst **7** for catalysis by creating coordinative unsaturation.

3.5. Mechanistic-based design of a new precatalyst (14).

Increasing the lability of the PPh_3 donor of precatalyst **7** could enhance transfer hydrogenation activity. Pyridine is thought to be more labile than PPh_3 on ruthenium,[50] and therefore could enhance the catalytic activity by increasing the coordinative unsaturation during catalysis by disassociating more readily from ruthenium than PPh_3. It was found that pyridine will replace PPh_3 as a ligand when **7** is stirred in neat pyridine for 3 h, accompanied by the gradual colour change from green to bright orange. A bright orange microcrystalline powder was isolated upon precipitation with cold pentane and was attributed to the bis-pyridine complex $RuCl(\eta^3\text{-dcpx})Py_2$ (**14**) (Figure 3.14).

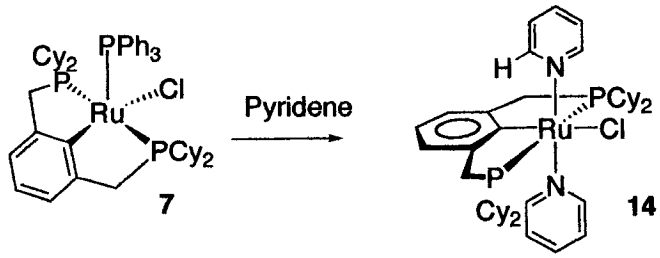

Figure 3.13. Formation of complex **14**.

The ^{31}P NMR spectrum of the material assigned as **14** showed the clean formation of a singlet at 42.36 ppm attributed to the two equivalent dcpx phosphines. The ^1H NMR spectrum displayed an uncharacteristic signal at δ 11.24 ppm attributed to ortho pyridine hydrogens above and below the benzene

ring in **14** (Figure 3.14), which are strongly deshielded when compared to the normal range for pyridine which is between 6 and 9 ppm, even in a related Ru-PCP(tpy) (tpy = terpyridine) complex [Ru(η^3dppx)(terpy)]Cl.[51] This difference could be due to the high steric congestion of **14**. This strongly deshielded proton, as well as the sharp features of the ^{1}H NMR spectrum of the pyridine rings in **14** suggests that they are fixed in one position by the bulky cyclohexyl groups of the dcpx ligand, and that the diamagnetic anisotropy of the benzene ring deshields the hydrogens on the locked pyridine rings. Although **14** is coordinatively saturated, it is predicted that upon activation it will be converted into a coordinatively unsaturated species more easily than **7**.

3.6. Conclusions.

A detailed mechanistic study of **7** was carried out in transfer hydrogenation catalysis. Interpretation of kinetics and in situ NMR data links **7**, **8a/b**, **9a/b**, **10**, and **12** in catalysis. One surprising conclusion of this work is that the active species is not an η^3-bound dcpx complex, but rather an η^2-PC(H)P-bound transient species **12**, in which the ruthenium-carbon bond has been thermally cleaved. We suggest the low enantioselectivity of chiral PCP complexes that have been reported[9] is due to the active species being a η^2-PC(H)P-bound entity, which would not have a rigid chiral pocket. Finally, **4a** and **7** show similar activity in transfer hydrogenation catalysis, which is not consistent with our initial hypothesis that the basic phosphine containing **7** would be more active for

transfer hydrogenation than **4a**. A possible explanation for this result is that both systems operate by a similar mechanism of catalysis, in which the formation of the active species through PCP carbon-ruthenium bond thermolysis has a stronger influence on activity than the phosphine donor basicity.

References

(1) Chaloner, P. A.; Esteruelas, M. A.; Joo, F.; Oro, L. A. *Homogeneous Hydrogenation.* Kluwer: Boston, 1994.

(2) Aranyos, A.; Csjernyik, G.; Szabó, K. J.; Bäckvall, J.-E. *J. Chem. Soc., Chem. Commun.* **1999**, 351.

(3) Albrecht, M.; Kocks, B. M.; Spek, A. L.; van Koten, G. *J. Organomet. Chem.* **2001**, *624*, 271.

(4) van der Boom, M. E.; Milstein, D. *Chem. Rev.* **2003**, *103*, 1759.

(5) Dani, P.; Karlen, T.; Gossage, R. A.; Gladiali, S.; van Koten, G. *Angew. Chem., Int. Ed.* **2000**, *39*, 743.

(6) Drouin, S. D., Ph. D. Thesis, University of Ottawa, 2004.

(7) Drouin, S. D.; Amoroso, D.; Yap, G. P. A.; Fogg, D. E. *Organometallics* **2002**, *21*, 1042.

(8) Noyori, R. *Journal of the American Chemical Society* **2003**, *125*, 13490.

(9) Albrecht, M.; van Koten, G. *Angew. Chem., Int. Ed.* **2001**, *40*, 3750.

(10) Gusev, D. G.; Dolgushin, F. M.; Antipin, M. Y. *Organometallics* **2000**, *19*, 3429.

(11) Gusev, D. G.; Madott, M.; Dolgushin, F. M.; Lyssenko, K. A.; Antipin, M. Y. *Organometallics* **2000**, *19*, 1734.

(12) Gusev, D. G.; Maxwell, T.; Dolgushin, F. M.; Lyssenko, M.; Lough, A. J. *Organometallics* **2002**, *21*, 1095.

(13) Reinhart, B.; Gusev, D. G. *New J. Chem.* **1999**, *23*, 1.

(14) van der Boom, M. E.; Kraatz, H.-B.; Hassner, L.; Ben-David, Y.; Milstein, D. *Organometallics* **1999**, *18*, 3873.

(15) Cross, R. J.; Kennedy, A. R.; Manojlovic-Muir, L.; Muir, K. W. *J. Organomet. Chem.* **1995**, *493*, 243-9.

(16) Cross, R. J.; Kennedy, A. R.; Muir, K. W. *J. Organomet. Chem.* **1995**, *487*, 227-33.

(17) Kennedy, A. R.; Cross, R. J.; Muir, K. W. **1995**, *231*, 195.

(18) Kennedy, A. R.; Cross, R. J.; Muir, K. W. **1995**, *231*, 207.

(19) Park, S. *Bull. Korean Chem. Soc.* **2002**, *23*, 132-136.

(20) Park, S. *Bull. Korean Chem. Soc.* **2000**, *21*, 1251.

(21) Seul, J. M.; Park, S. *J. Chem. Soc., Dalton Trans.* **2002**, 1153.

(22) Yun, J. G.; Seul, J. M.; Lee, K. D.; Kim, S.; Park, S. *Bull. Korean Chem. Soc.* **1996**, *17*, 311.

(23) Amoroso, D. Ph. D. Thesis, University of Ottawa, 2002.

(24) Amoroso, D.; Jabri, A.; Yap, G. P. A.; Gusev, D. G.; dos Santos, E. N.; Fogg, D. E. *Organometallics* **2004**, *23*, 4047.

(25) Farrington, E. J.; Viviente, E. M.; Williams, B. S.; van Koten, G.; Brown, J. M. *J. Chem. Soc., Chem. Commun.* **2002**, 308.

(26) Vigalok, A.; Uzan, O.; Shimon, L. J. W.; Ben-David, Y.; Martin, J. M. L.; Milstein, D. *J. Am. Chem. Soc.* **1998**, *120*, 12539.

(27) Crocker, C.; Errington, R. J.; McDonald, W. S.; Odell, K. J.; Shaw, B. L.; Goodfellow, R. J. *J. Chem. Soc., Chem. Commun.* **1979**, 498.
(28) Crocker, C.; Errington, R. J.; Markham, R.; Moulton, C. J.; Odell, K. J.; Shaw, B. L. *J. Am. Chem. Soc.* **1980**, *102*, 4373.
(29) March, J. *Advanced Org. Chem. 3rd Ed.* 1985.
(30) Ponndorf, W. *Angew. Chem.* **1926**, 138.
(31) Berkessel, A.; Schubert, T. J. S.; Mueller, T. N. *J. Am. Chem. Soc.* **2002**, *124*, 8693.
(32) Walling, C.; Bollyky, L. *J. Am. Chem. Soc* **1964**, *86*, 3750.
(33) Bäckvall, J.-E. *J. Organomet. Chem.* **2002**, *652*, 105.
(34) LePage, M. D.; James, B. R. *J. Chem. Soc., Chem. Commun.* **2000**, 1647.
(35) Poyatos, M.; Mata, J. A.; Falomir, E.; Crabtree, R. H. *Organometallics* **2003**, *22*, 1110.
(36) Louie, J.; Bielawski, C. W.; Grubbs, R. H. *J. Am. Chem. Soc.* **2001**, *123*, 11312.
(37) Crabtree, R. H. *Organometallics* **2003**, *22*, 1110-1114.
(38) They report 65% conversion of acetophenone within 4 h at 34 mol % NaOH.
(39) While the presence of base can trigger aldol condensation of ketones, only traces of heavier byproducts (<< 1%) were observed even over the combined timescale of pretreatment and reduction experiments (ca. 3.5 h), reaching 3% after 19 h.
(40) Chowdhury, R.; Bäckvall, J.-E. *J. Chem. Soc., Chem. Commun.* **1991**, 1063.
(41) Morton, D.; Cole-Hamilton, D. J. *J. Chem. Soc., Chem. Commun.* **1988**, 1154.
(42) Amoroso, D.; Yap, G. P. A.; Fogg, D. E. *Can. J. Chem.* **2001**, *79*, 958.
(43) Liu, S. H.; Ng, S. M.; Wen, T. B.; Zhou, Z. Y.; Lin, Z.; Lau, C. P.; Jia, G. *Organometallics* **2002**, *21*, 4281.
(44) Kubas, G. J. *Metal Dihydrogen and σ-Bond Complexes. Structure, Theory and Reactivity*. Kluwer Academic/Plenum Publishers: New York, 2001.
(45) Sandhu, S. S.; Mehta, A. K. *Indian J. Chem.* **1974**, *12*, 834.
(46) Amoroso, D.; Fogg, D. E. *Macromolecules* **2000**, *33*, 2815.
(47) Whittlesey, M. K.; Perutz, R. N.; Virrels, I. G.; George, M. W. *Organometallics* **1997**, *16*, 268.
(48) Grushin, V. *Chem. Rev.* **2004**, *104*, 1629-1662.
(49) Stoop, R. M. *Organometallics* **2000**, *19*, 4117.
(50) Love, J. A.; Morgan, J. P.; Trnka, T. M.; Grubbs, R. H. *Angew. Chem., Int. Ed.* **2002**, *41*, 4035.
(51) Karlen, T.; Dani, P.; Grove, D. M.; Steenwinkel, P.; van Koten, G. *Organometallics* **1996**, *15*, 5687.

Chapter 4

Synthesis of chelating ligands containing pyrrole and highly basic donors.

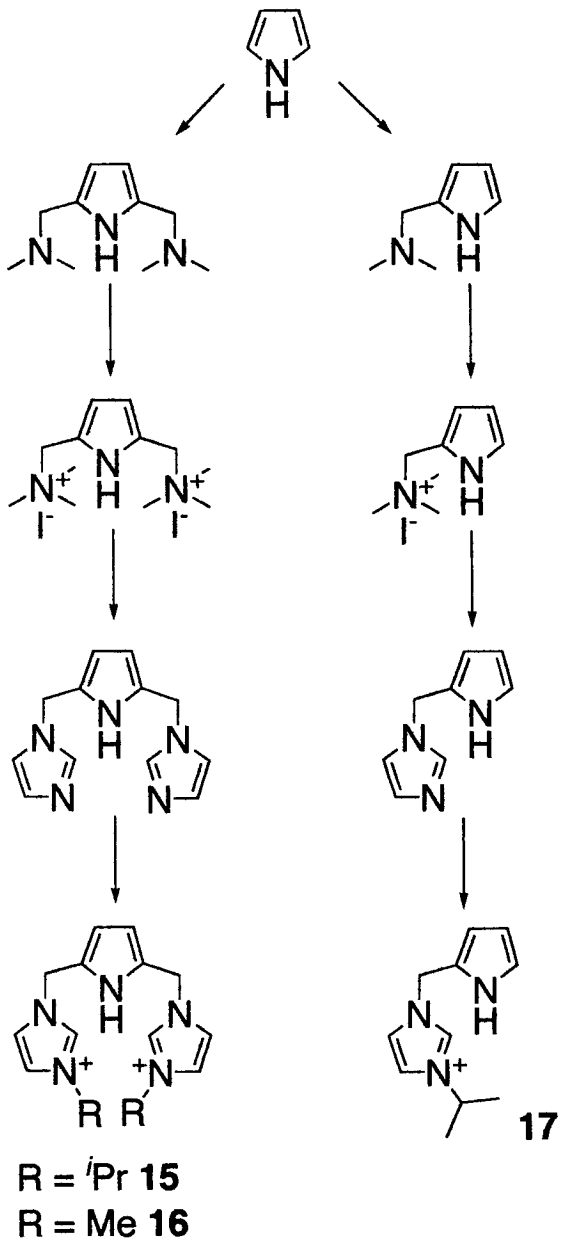

Figure 4.1. Pictorial summary of chapter 4.

4.1. Introduction.

Chapter 1 discusses the importance of ligands in homogeneous catalysis. In the case of homogeneous ruthenium catalysts for olefin metathesis[1,2] and hydrogenation,[3] highly basic, bulky, chelating ligands have been reported to enhance activity and selectivity. This enhancement could be due to stabilization of coordinatively unsaturated catalytic intermediates.[4-6]

Olefin metathesis is a very important catalytic transformation which has become more practical with the development of the air and moisture resistant Grubbs catalyst, $RuCl_2(PCy_3)_2(=CHPh)$ (Figure 4.2 a).[7] Following this discovery, an intense research effort in the past few years has focused on enhancements of this first generation catalyst, including the use of a highly basic N-heterocyclic carbene (NHC) ligand "second generation" Grubbs catalyst (Figure 4.2 b).[2,8,9] A chiral chelating NHC ligand has also been used (Figure 4.2 c).[10]

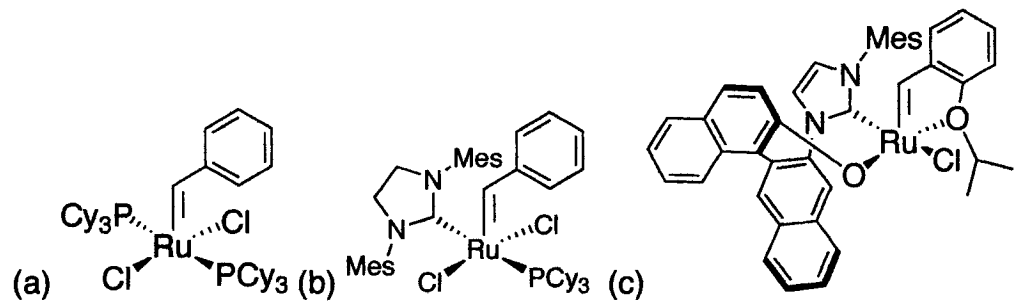

Figure 4.2. Progression of ligand systems applied to olefin metathesis (a) Grubbs catalyst (b) Second generation Grubbs catalyst (c) chiral bidentate system. (Mes = Mesityl)

Further improvements could be possible with mechanistic understanding of this catalyst system. For example, our group reported that ruthenium alkylidenes deactivate by formation of a face-bridged dimer (Figure 4.3),[11,12]

which led us to explore the possibility that incorporation of "pseudohalide" anionic donors could prevent this deactivation pathway. The replacement of the chloride ligands of Grubbs catalyst by us[13,14] and others[15] with a pseudohalide ligand to generate $RuX_2(PCy_3)_2(=CHPh)$ (X = perfluorophenoxide, carboxylate) results in increased catalyst lifetime.

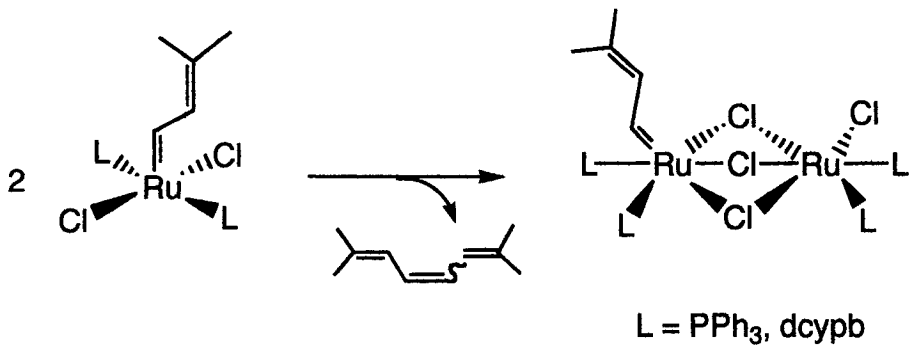

Figure 4.3. Bimolecular deactivation of ruthenium alkylidenes through formation of a stable face-bridged chloride dimer.

Future improvements in catalytic performance could be made by incorporation of a pseudohalide into a highly basic chelating ligand framework. In addition, such a chelating system could provide a robust scaffold to explore potentially useful tandem catalysis transformations,[16] such as tandem olefin metathesis-hydrogenation, developed by our group[17] and others.[18] Toward this goal, Dino Amoroso of our group discovered that the reaction of dcpx with the ruthenium alkylidene $RuCl_2(PPh_3)_2(=CHR)$ generated the agostic complex $RuCl_2(\eta^2\text{-dcpx})(=CHR)$ (Figure 4.4a).[19] The aryl C-H bond of this complex is not activated to form an η^3-bound ligand, even in the presence of a strong base. In

related work, the research group of Jia[20,21] has reported the reactivity of an alkylidene ligand on ruthenium pincer complexes, and found that the aryl carbanion of dppx inserts into the ruthenium alkylidene bond (Figure 4.4 b), suggesting the PCP ligand carbanion is too basic, and possibly inserts into the ruthenium alkylidene.

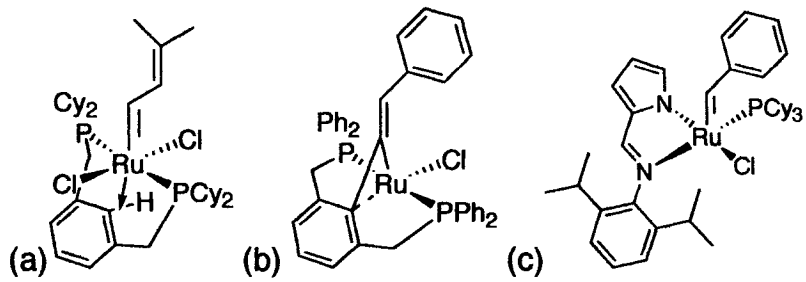

Figure 4.4. (a) Fogg's PCP alkylidene (b) Jia's η^4 bound pincer (c) Fogg's pyrrolide alkylidene.

An improved ligand would incorporate a less basic anionic donor, which would therefore be less likely to insert into the ruthenium alkylidene. An anionic donor with the correct geometry to incorporate into a tridentate motif would be the pyrrolide anion, in which the pyrrole N-H proton has an acidity (pKa = 16) similar to alcohols.[22] It was discovered by Samantha Drouin[23,24] of our group that a known imino-pyrrolato ligand can successfully be installed as a chelating anionic donor on a ruthenium alkylidene to form Ru(NN)Cl(PCy_3)(=CHPh) (NN = iminopyrrolato) (Figure 4.4 c). This supports the suggestion that a less basic anionic donor would be more compatible with the ruthenium alkylidene functionality. Furthermore, this catalyst system is similar to those incorporating

Schiff-base ligands, with the same advantage of high air and moisture stability, and the disadvantage of a lower activity than even the first generation Grubbs catalyst. Our group reported that the imino-pyrrolato catalyst system requires oxygen for activation, which was suggested to open an active site by oxidation of the bound PCy_3. This requirement for phosphine oxidation for activity is possibly due to the strong affinity of PCy_3 to the ruthenium center. A more strongly donating ligand than the imine nitrogen of $Ru(NN)Cl(PCy_3)(=CHPh)$ would make the ruthenium center more electron rich, thus activating it towards metathesis. A novel bidentate or tridentate ligand utilizing pyrrole and a stronger donor such as a NHC or basic phosphine could provide such a highly reactive catalyst system.

Discussed in this chapter is the synthesis and characterization of ligand precursors in which strongly donating NHC donors are incorporated into a chelating framework. The new design is a bidentate carbene-pyrrole (Figure 4.5 a) or tridentate carbene-pyrrole-carbene (Figure 4.5 b) ligand in which the geometry is meridionally coordinating to the metal center, similar to chelating carbene-alcohol ligands that have been reported,[10,25] and the porphyrin class of ligands.[26]

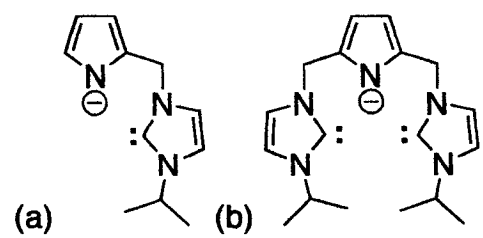

Figure 4.5. Designs for CN type ligand (a) and CNC (b).

4.2. Synthesis of Imidazolium Ligand Precursors.

Tridentate CNC ligand precursors **15** and **16** were obtained in 70 % and 80 % overall yield respectively, in a synthesis starting from pyrrole (Figure 4.6). The selective Mannich dimethylamino-methylation of pyrrole in water with formaldehyde and dimethylammonium chloride yields 2,5-bis[(dimethylamino)methyl]-pyrrole with high selectivity. Subsequent quaternization of the dimethylamino groups with methyl iodide forms 2,5-bis[(trimethylammonium)methyl]-pyrrole diiodide.[27] This strategy is based on work reported by the research group of Elsenbaumer, which demonstrated that this ammonium derivative is particularly suited to further functionalization by nucleophilic displacement of trimethylamine with phenylthiolate.[27] Accordingly, displacement of trimethylamine with imidazole forms 2,5-bis[(imidazol)methyl]-pyrrole.[28]

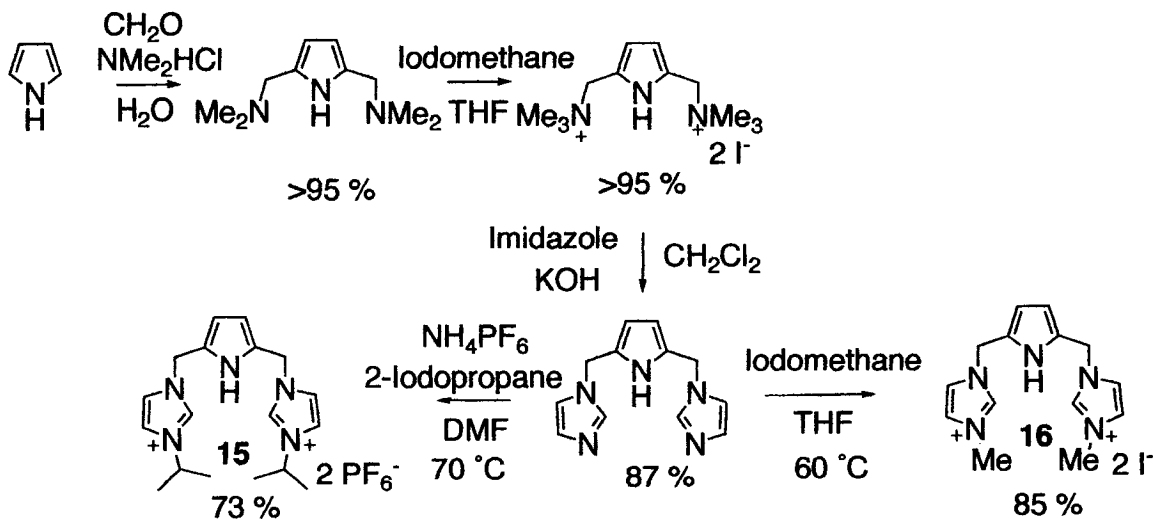

Figure 4.6. Synthesis of CNC ligand precursors **15** and **16**.

Treatment of a DMF solution of 2,5-bis[(imidazole)methyl]-pyrrole with 3 equivalents of 2-iodopropane at 70 °C for 1 hr yields 2,5-bis[(isopropylimidazolium)methyl]-pyrrole diiodide (as judged by TLC and NMR analysis of an aliquot of the crude reaction mixture). The solution turns light brown over the course of the reaction, probably due to some decomposition of the thermally sensitive pyrrole ring. A water-insoluble purple byproduct (probably a poly(pyrrole) species) can be removed by filtration through Celite. The remaining clear solution was added drop-wise to an aqueous solution containing 2 equivalents of NH_4PF_6, upon which a fine white solid forms, which was filtered off and dried to yield the white solid **15**. Thermally sensitive **15** is soluble only in polar organic solvents such as DMSO and DMF.

^{1}H NMR analysis of **15** (figure 4.7) reveals a triplet (J_{HH}= 2.5 Hz) integrating to one proton at δ 11.32 ppm a location characteristic of the pyrrole N-H proton.[29] Disappearance of this signal on addition of D_2O to the NMR sample further confirms this assignment, as does the absence of an HMQC correlation with any carbon signal. HMBC experiments reveal two and three-bond correlations to pyrrole ring *C*2 and *C*3, respectively. The remaining pyrrole ring protons, *H*3, appear as a doublet at δ 6.20 ppm (J_{HH}= 2.5 Hz, 2H). The quaternary carbons (*C*2) on the pyrrole ring provide a signal in the $^{13}C\{^1H\}$ NMR spectrum at δ 126.5 ppm, confirmed by the absence of only this signal in the DEPT-130 spectrum. The singlet at 5.30 ppm is assigned to the methylene protons, which was confirmed by direct coupling (by HMQC) to the only carbon

that had an even number of protons (signal down in the DEPT 130). The signal at 9.15 ppm (pseudo-t, imid-*H*1, J_{HH}= 2.5 Hz, 2H), is characteristic of imidazolium, which correlates to the two other chemically distinct protons the imidazolium ring by COSY (with the same coupling constant for both). The remaining imidazolium protons provide signals at δ 7.65 ppm (pseudo-t, imid-*H*4, J_{HH}= 2.5 Hz, 2H) and δ 7.88 ppm (pseudo-t, imid-*H*3, J_{HH}= 2.5 Hz, 2H), assigned by long-distance coupling (HMBC) to the isopropyl and methylene carbon, respectively. The A_6B system of the isopropyl group reveals the characteristic doublet at 1.45 ppm ($(CH_3)_2CH$, J_{HH}= 7 Hz, 12H) and septet at 4.63 ppm ($(CH_3)_2CH$, J_{HH}= 7 Hz, 2H). IR analysis reveals a characteristic N-H stretching band at 3389 cm^{-1}. The ESI mass spectrum shows the largest mass peak at 458 m/z corresponding to the loss of one PF_6^- anion from **15**. Elemental analysis were not collected due to lack of time.

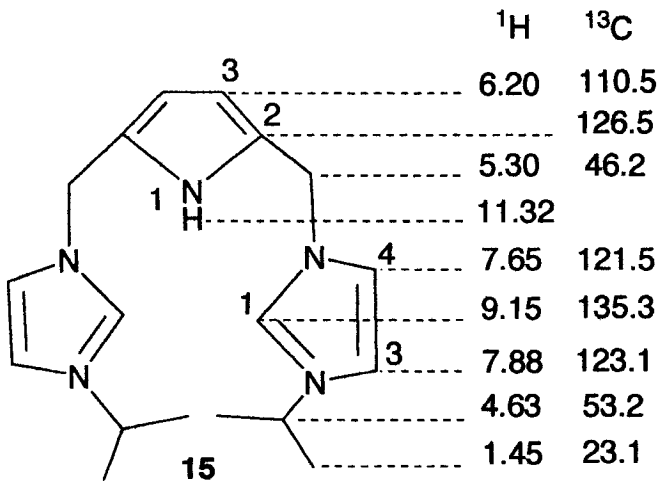

Figure 4.7. NMR analysis of **15**.

Less sterically demanding precursor **16** is synthesized by the same route as **15** (Figure 4.6). The structure of **16** was confirmed by ^{1}H and ^{13}C NMR analysis (Figure 4.8). The IR spectrum of **16** also reveals a characteristic NH stretch at 3390 cm^{-1}, and the ESI mass spectrum shows the highest mass peak at 384 m/z corresponding to loss of the iodide counter ion from **16**.

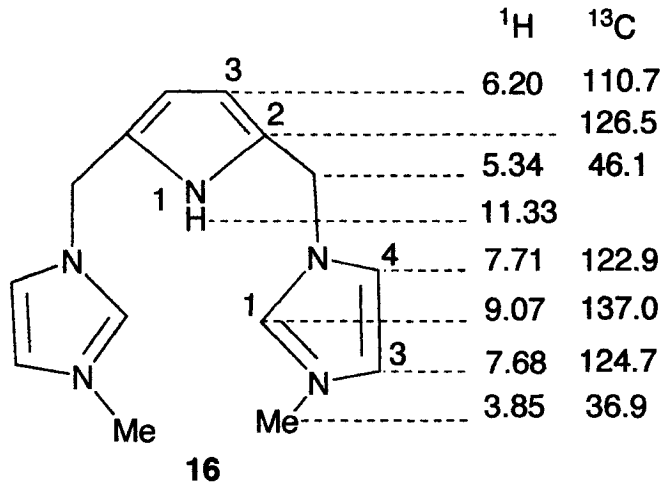

16

Figure 4.8. NMR analysis of **16**.

The bidentate ligand precursor 2-[(isopropylimidazolium)methyl]-pyrrole tetraphenylborate **17** was also synthesized by the same method used to synthesize **15**, with the only difference in the counterion being $B(Ph)_4^-$ in the case of **17** (Figure 4.9). The structure of **17** was confirmed by ^{1}H and ^{13}C NMR analysis (Figure 4.9). IR analysis shows a characteristic N-H stretching band at 3389 cm^{-1}. ESI mass spectrum shows the largest mass peak at m/z corresponding to loss of one $B(Ph)_4^-$ anion from **17**.

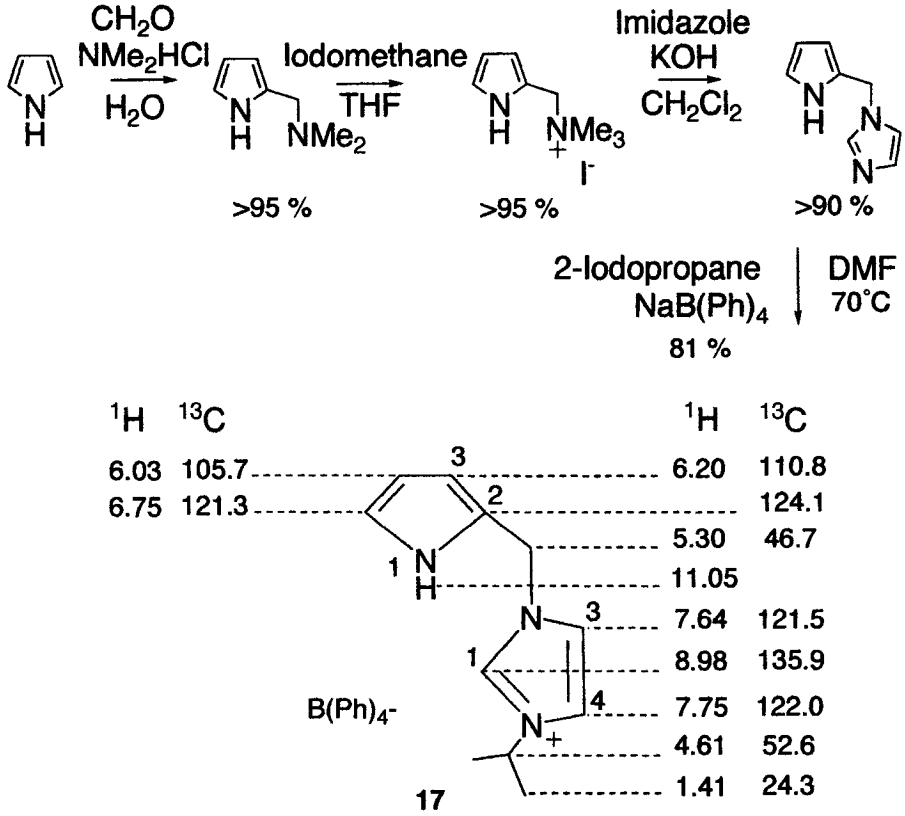

Figure 4.9. Synthesis and NMR analysis of **17**.

The attempts to generate free carbenes from the imidazolium salts **15-17** by deprotonation with the strong bases KH, KO^{t}Bu, or KN(SiMe$_3$)$_2$ failed. Addition of base to a suspension of the ligand precursor in dry, degassed THF resulted in the immediate formation of a deep red solution, possibly indicating double bond isomerization to form a conjugated, porphyrinogen-like chromophore.[30] The formation of a conjugated porphyrinogen-type product is supported by the observed loss of the characteristic methylene, imidazolium and pyrrole signals of **15** upon addition of base. Attempts at direct metalation of **15-17** with ruthenium(II), silver(I), and palladium(II) precursors always resulted in the

formation of dark red solutions of the ligand byproducts and sometimes ruthenium, silver or palladium black.

4.3. Conclusions.

In conclusion, chelating mono- and di-imidazolium pyrrole complexes were synthesized and characterized. Unfortunately, the free carbenes could not be obtained by deprotonation (possibly due to double-bond isomerization), nor could the metal complexes be obtained via direct metalation. However, substitution at the methylene positions of the proligand (see Figure 4.10) may circumvent isomerization, and permit isolation of stable free carbenes.

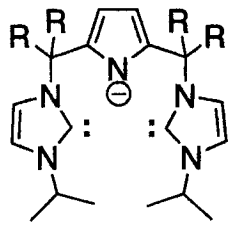

Figure 4.10. A possible improved version of carbene-pyrrole-carbene ligand with R= alkyl or aryl in the methylene position.

References

(1) Cucullu, M. E.; Li, C.; Nolan, S. P.; Ngyuen, S. T.; Grubbs, R. H. *Organometallics* **1998**, *17*, 5565.

(2) Weskamp, T.; Kohl, F. J.; Hieringer, W.; Gleich, D.; Herrmann, W. A. *Angew. Chem., Int. Ed.* **1999**, *38*, 2416.
(3) Lee, H. M.; Smith, D. C.; He, Z.; Stevens, E. D.; Yi, C. S.; Nolan, S. P. *Organometallics* **2001**, *20*, 794.
(4) van der Boom, M. E.; Milstein, D. *Chem. Rev.* **2003**, *103*, 1759.
(5) Vigalok, A.; Milstein, D. *Acc. Chem. Res.* **2001**, *34*, 798.
(6) Albrecht, M.; van Koten, G. *Angew. Chem., Int. Ed.* **2001**, *40*, 3750.
(7) Trnka, T. M.; Grubbs, R. H. *Acc. Chem. Res.* **2001**, *34*, 18.
(8) Huang, J.; Schanz, H.-J.; Stevens, E. D.; Nolan, S. P. *Organometallics* **1999**, *18*, 5375.
(9) van Veldhuizen, J. J.; Garber, S. B.; Kingsbury, J. S.; Hoveyda, A. H. *J. Am. Chem. Soc.* **2002**, *124*, 4954.
(10) Tsang, W. C. P.; Hultzsch, K. C.; Alexander, J. B.; P. J. Bonitatebus, J.; Schrock, R. R.; Hoveyda, A. H. *J. Am. Chem. Soc* **2003**, *125*, 2652.
(11) Amoroso, D.; Snelgrove, J. L.; Conrad, J. C.; Drouin, S. D.; Yap, G. P. A.; Fogg, D. E. *Adv. Synth. Catal.* **2002**, *344*, 757.
(12) Amoroso, D.; Yap, G. P. A.; Fogg, D. E. *Organometallics* **2002**, *21*, 3335.
(13) Conrad, J. C.; Amoroso, D.; Czechura, P.; Yap, G. P. A.; Fogg, D. E. *Organometallics* **2003**, *22*, 3634.
(14) Conrad, J. C.; Parnas, H.; Snelgrove, J. L.; Fogg, D. E. *J. Am. Chem. Soc* **2005**, accepted.
(15) Krause, J. O.; Zarka, M. T.; Anders, U.; Weberkskirch, R.; Nuyken, O.; Buckmeiser, M. R. *Angew. Chem.* **2003**, *115*, 6147.
(16) Drouin, S. D.; Zamanian, F.; Fogg, D. E. *Organometallics*, *20*, 5495. (b) Drouin, S. D.; Yap, G. P. A.; Fogg, D. E. *Inorg. Chem.* **2000**, *39*, 5412. (c) Fogg, D. E.; Drouin, S. D.; Zamanian, F. U. S. Patent 6,486,263.
(17) Drouin, S. D.; Zamanian, F.; Fogg, D. E. *Organometallics* **2001**, *20*, 5495.
(18) Louie, J.; Bielawski, C. W.; Grubbs, R. H. *J. Am. Chem. Soc.* **2001**, *123*, 11312.
(19) Amoroso, D. Ph. D. Thesis, University of Ottawa, 2002.
(20) Lee, H. M.; Yao, J.; Jia, G. *Organometallics* **1997**, *16*, 3927.
(21) Jia, G.; Lee, H. M.; Xia, H. P.; Williams, I. D. *Organometallics* **1996**, *15*, 5453.
(22) March, J. *Advanced Org. Chem. 3rd Ed.* 1985.
(23) Drouin, S. D., Ph. D. Thesis, University of Ottawa, 2004.
(24) Drouin, S. D.; Foucalt, H. F.; Yap, G. P. A.; Fogg, D. E. *Can. J. Chem.* **2005**, in press.
(25) Arnold, P. L.; Scarisbrick, A. C. *Organometallics* **2004**, *23*, 2519.
(26) J.L. Sessler, A. G., V Kral and V. Lynch *Inorg. Chem.* **1996**, *35*, 6636.
(27) I. T. Kim, R. L. E. *Chem. Commun.* **1998**, 327.
(28) I. T. Kim, R. L. E. *Tet. Lett.* **1998**, *39*, 1087.
(29) A. Jasat, D. D. *Chem. Rev.* **1997**, *97*, 2267-2340.
(30) Mazet, C.; Gade, L. H. *Inorg. Chem.* **2003**, *42*, 210.

CHAPTER 5

Transfer Hydrogenation Involving Ruthenium Secondary Phosphine Complexes

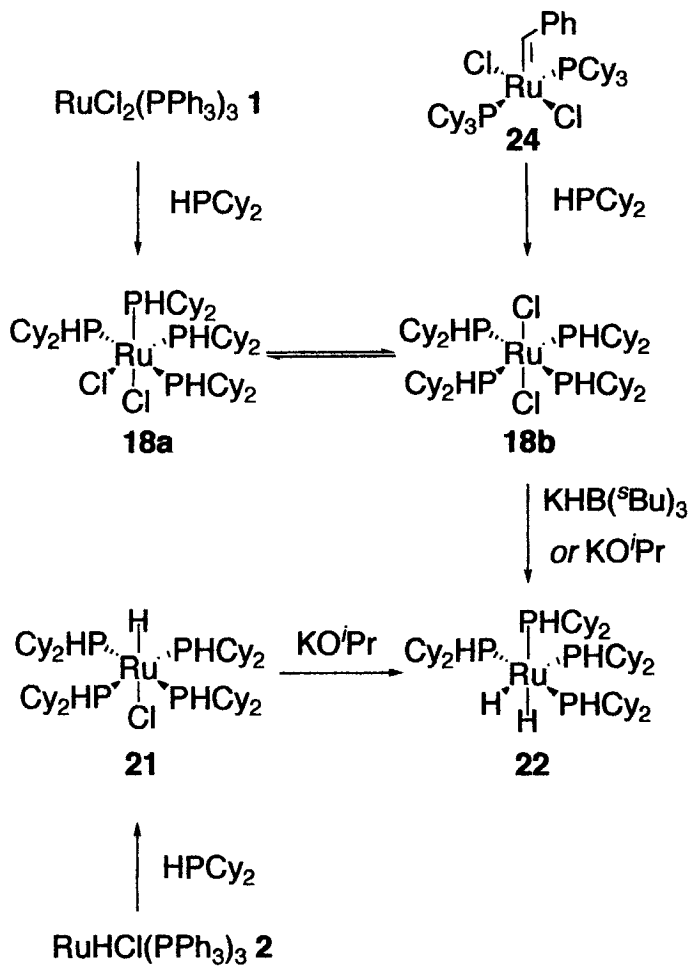

Figure 5.1. Pictorial Summary of Chapter 5.

5.1. Introduction.

The importance of new ligand design in catalysis was discussed in Chapter 1. Biological enzymes are extremely active in catalysis.[1] Many highly efficient metallo-enzymes utilize cooperative interactions between one or more acidic/basic sites in the outer coordination sphere of the transition metal center to activate substrates and enhance selectivity (Figure 5.2).

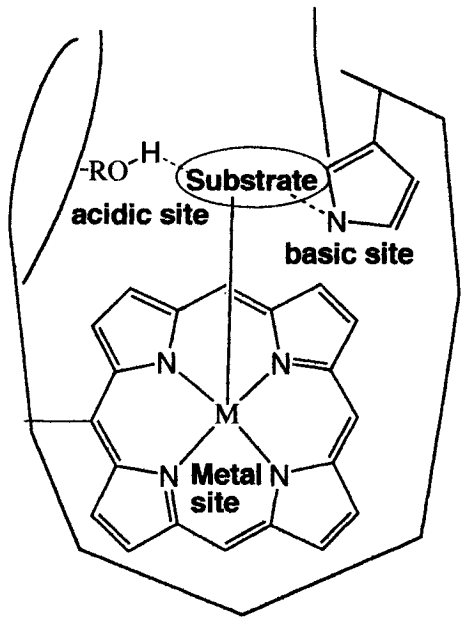

Figure 5.2. Enzyme's active site, utilizing cooperative interactions with acidic and basic sites to activate a substrate.

One way in which to develop and improve synthetic homogeneous catalysts would be to incorporate acidic and/or basic sites in the outer sphere, akin to natural metallo-enzymes. One famous example of research in this direction is Noyori's highly active ketone hydrogenation catalyst, RuH_2(dppe)(en), which contains a diamine ligand providing acidic sites in the outer sphere of the metal center.[2,3] Mechanistic studies revealed that the enhancement of catalysis

occurs via an outer-sphere activation of the ketone oxygen through hydrogen bonding with the amine (Figure 5.3).[4-7]

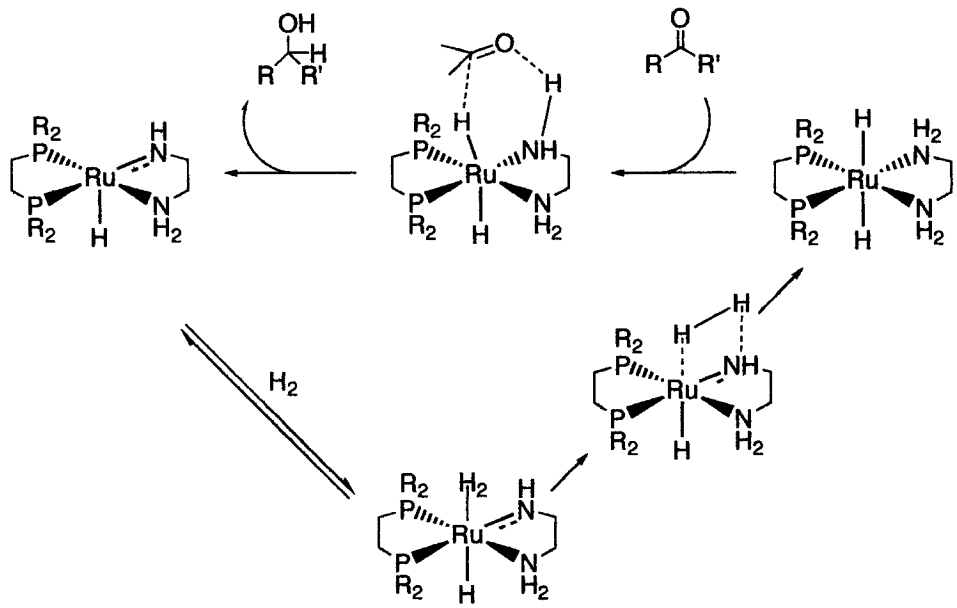

Figure 5.3. Mechanism of the Noyori system which operates through hydrogen bonding.[4,7]

As phosphine ligands (soft donor, pi back-bonding) play a larger role in catalysis with late transition metals than nitrogen-based ligands (hard donor, no pi back-bonding),[8] it would be interesting to consider the potential of utilizing primary and secondary phosphine donors in analogy to the nitrogen donors in the Noyori catalyst system. In addition to catalytic applications, the investigation of the nature of potential protic-hydridic interactions between ruthenium hydrides and acidic phosphine protons is of fundamental importance.

Such chemistry has not been intensively investigated in the past, as these ligands are thought to be unstable towards deprotonation and oligomerization.

This is surprising considering a quantitative study has reported a stronger phosphine-ruthenium bond strength (an important characteristic in preventing deactivation of catalytic species) in secondary phosphines than the corresponding tertiary phosphines.[5] Traditionally, phosphines have been evaluated on their basicity and steric bulk alone, as a transition metal's electron-richness is well known to be directly linked to phosphine basicity and cone angle,[9] but consideration of other important properties such as acidic sites could increase the versatility of phosphine ligands in catalysis.

One systematic study has reported that pendent hydrogen atoms, when attached directly to the phosphorus atoms, have a pronounced and unique positive effect on the rates of CO dissociation from $Ru(CO)_4L$ (L = secondary/primary phosphine) complexes, compared to the complexes of corresponding tertiary phosphines. Significant kinetic isotope effects on CO dissociation by the pendant hydrogen atom were reported,[10] which is associated with occurrence of direct Ru–H or Ru–P–H agostic bond making as the CO ligand departs from the ruthenium.

Recently, secondary phosphines have been highlighted for their enhanced activities over even bulky tri-alkyl phosphines for palladium catalyzed coupling reactions, in which activity is greatly enhanced by strongly bound ligands.[11] One reported catalytic study of ruthenium-secondary phosphine complexes was in atom transfer radical polymerization (ATRP), in which the ligand $HPCy_2$ generates a much less active catalyst than PCy_3. This was suggested to be due

to a smaller cone angle (143°) and weaker basicity (p*Ka* $H_2PCy_2^+$ = 4.55) compared to the highly basic PCy_3 (170°, p*Ka* $HPCy_3^+$ = 9.70).[12]

The P-H bond is a major benefit in elucidating the nature of ruthenium-secondary phosphine interactions by NMR and IR analysis. Both the phosphorus and hydrogen nuclei are close to 100% abundant spin 1/2 nuclei with large sensitivities, and ruthenium complexes of primary and secondary phosphines exhibit many characteristic NMR chemical shifts ($^{31}P\{^1H\}$ Ru*P*H = δ_P 50 to –50 ppm; ^1H RuP*H* = δ_H 4-6 ppm, $^1J_{PH}$ = *300* Hz), and IR signals (*v* P-H = 2300-2400 cm^{-1}).[13]

In this chapter is reported the synthesis and catalytic studies of ruthenium primary/secondary phosphine complexes in transfer hydrogenation.

5.2. Synthesis of primary and secondary phosphine complexes.

The previously reported $RuCl_2L_4$ complexes[13] of the phosphine ligands $HPCy_2$, $HPPh_2$, and H_2PPh were synthesized to study the effect of phosphine acidity and cone angle on catalytic activity. This was accomplished by reaction of $RuCl_3$ and six equivalents of the phosphine ligand in refluxing methanol for several hours. All the complexes, $RuCl_2L_4$ (L = $HPCy_2$ **18a/b**, $HPPh_2$ **19a/b**, and H_2PPh **20a/b**) exist as both the cis (**18a-20a**) and trans (**18b-20b**) isomers in solution, with greater amounts (~90% by NMR analysis) of the trans isomers,[13] indicating that these are the thermodynamically most stable isomers (Figure 5.4).

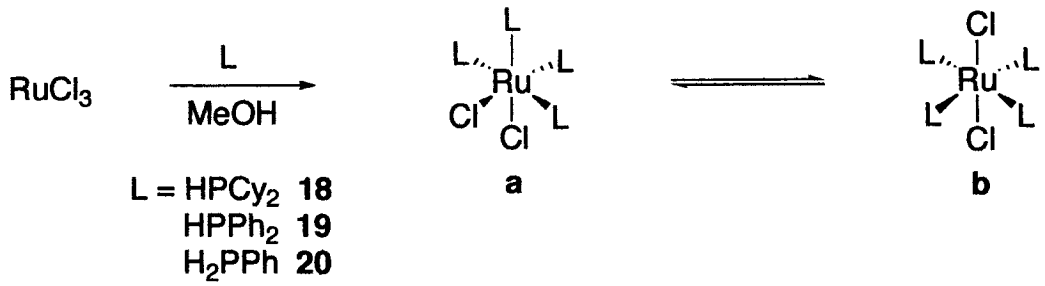

Figure 5.4. Synthesis of complexes **18a/b-20a/b**.

Isomerization between the cis and trans isomers of **18a/b**, **19a/b**, or **20a/b** in solution to yield equilibrium mixtures is very slow at room temperature, on the order of days.[13] This suggests that the barrier to isomerization from cis to trans (possibly occurring through a disassociative mechanism) is relatively large. Reaction of $RuCl_2(PPh_3)_3$ **1**, with four equivalents of $HPCy_2$ yields predominantly the cis isomer **18a** (>95% by in situ $^{31}P\{^1H\}$ NMR analysis minutes after addition of $HPCy_2$). This indicates that the trans isomer **18b** is more stable, and cis **18a** is the kinetic product. This is of interest because the cis and trans isomers may exhibit differing reactivity.

As ruthenium hydrides are probably the active species in transfer hydrogenation, as discussed in Chapter 3, synthesis of the monohydride and dihydride derivatives of **18a/b** was undertaken. Addition of four equivalents of $HPCy_2$ to $RuHCl(PPh_3)_3$ (**2**) in benzene results in the decolourization of the initially purple solution, accompanied by the formation of the monohydride $RuHCl(HPCy_2)_4$ **21** (Figure 5.5a). This is confirmed by ^1H NMR analysis. A single, characteristic pentet integrating one proton appears at δ_H –19.94 ppm ($^2J_{PH}$ = 14

Hz). The multiplicity confirms coupling to four equivalent phosphine ligands (which appear as a singlet at δ_P 35.66 ppm in the $^{31}P\{^1H\}$ NMR spectrum). ^{31}P-decoupling causes the hydride pentet to collapse to a singlet.

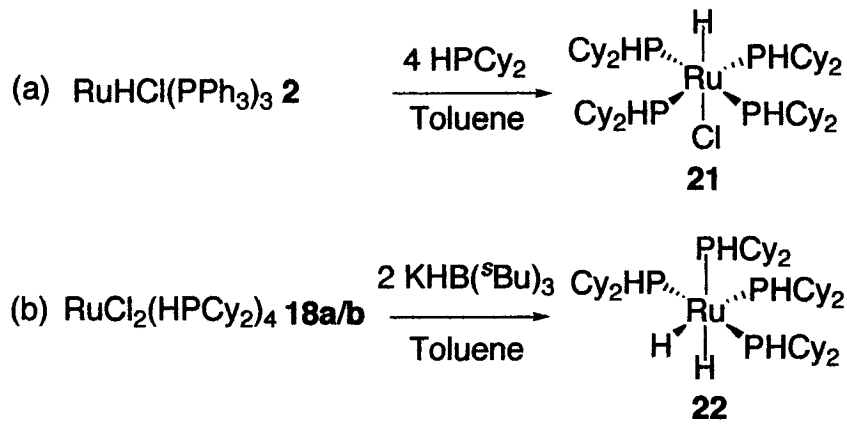

Figure 5.5. (a) Synthesis of monohydride **21**, and (b) dihydride **22**.

The cis isomer of dihydride **22** was also prepared. Addition of two equivalents of $KHB(^sBu)_3$ to **18a/b** in benzene decolourizes the initially yellow solution within minutes. ^{31}P NMR analysis reveals two sets of triplets at δ_P 50.70 and 38.8 ppm ($^2J_{PP}$ = 22 Hz) in a 1:1 ratio. This A_2B_2 system is consistent with the formulation of the product as cis dihydride **22** (Figure 5.5b). This complex was isolated by precipitation with hexanes to give a white microcrystalline powder, which is awaiting further characterization.

In an attempt to synthesize a dihydride of a ruthenium phenylphosphine containing complex, $KHB(^sBu)_3$ was added to a solution of **20a/b** in benzene (Figure 5.6), and a color change from yellow to red is observed, along with moderate bubbling indicating the loss of H_2 gas. The $^{31}P\{^1H\}$ NMR analysis

reveals the appearance of very broad (~20 ppm) signals centered at δ_P –140 ppm, which may indicate a heterogeneous mixture of paramagnetic bridging phosphido species. This result is possibly due to protic-hydridic interactions between a transient ruthenium hydride species and the protons on H_2PPh, favoring the loss of H_2 gas (Figure 5.6).

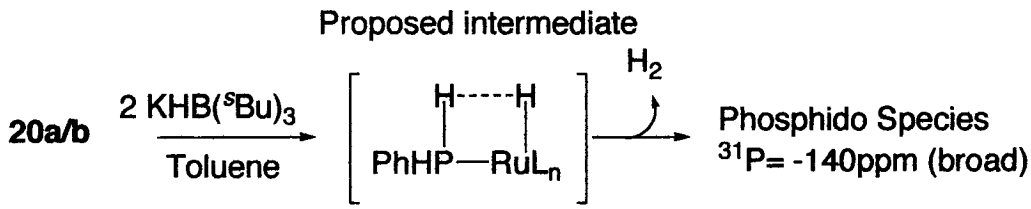

Figure 5.6. Reaction of $KHB(^sBu)_3$ with **20a/b**.

To further the fundamental understanding of the nature of the interactions of primary phosphines and ruthenium hydrides, use of the well-defined, highly basic dcpx ligand would provide a useful platform to build the chemistry of primary and secondary phosphines on ruthenium. Upon addition of two equivalents of H_2PPh to $RuCl(\eta^3\text{-PCP})PPh_3$ (**3**) in toluene, the initially dark green solution went instantly light yellow. We identify the product $RuCl(\eta^3\text{-PCP})(PH_2Ph)_2$ **23** on the basis of NMR studies (Figure 5.7).

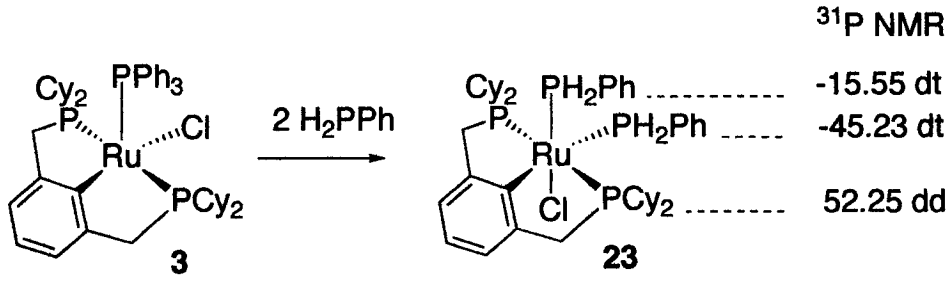

Figure 5.7. Synthesis and ^{31}P NMR of **23**.

The in situ ^{31}P NMR spectrum of **23**, shows a characteristic A_2BC system for the three chemically distinct phosphine nuclei. They are assigned as the two equivalent PCP phosphines centered at δ_P 52.25 ppm (2P, dd $^2J_{PP}$ = 34 Hz, $^2J_{PP}$ = 20 Hz, PCP), the less shielded PH_2Ph trans to chloride anion at δ_P -15.55 ppm (1P, dt, $^2J_{PP}$ = 34 Hz, $^2J_{PP}$ = 19 Hz, $^1J_{PH}$ = 319 Hz, PH_2Ph), and the more shielded PH_2Ph trans to the strongly donating aryl carbanion δ_P -45.23 ppm (1P, dt, $^2J_{PP}$ = 20Hz, $^2J_{PP}$ = 19 Hz, $^1J_{PH}$ = 304 Hz, PH_2Ph). The proton-coupled ^{31}P NMR spectrum reveals no coupled protons for the signal due to the PCP ligand, while the two peaks assigned to the PH_2Ph groups were coupled to protons, leading to a complex splitting pattern (broad triplets result from the large P-H coupling constant of 300 Hz). The way is open for future mechanistic studies on hydride derivatives of **23**. One result of mechanistic interest is that the highly basic aryl carbanion in the PCP ligand of **23** is stable against deprotonation of a nearby PH_2Ph ligand at room temperature.

Hydrophosphination involves formation of a carbon-phosphorus bond. An opportunity to study secondary phosphines in tandem catalyst transformations arose due to the high activity of **18a/b** in transfer hydrogenation (see later). The

products of reaction of the Grubbs Catalyst $RuCl_2(PCy_3)_2(=CHPh)$ (**24**) with $HPCy_2$ may give insight into what opportunities lay in tandem metathesis-hydrogenation for this ligand. Addition of five equivalents of $HPCy_2$ to **24** in benzene caused the initially purple solution to turn to clear yellow over 20 minutes at room temperature forming **18b** (Figure 5.8).

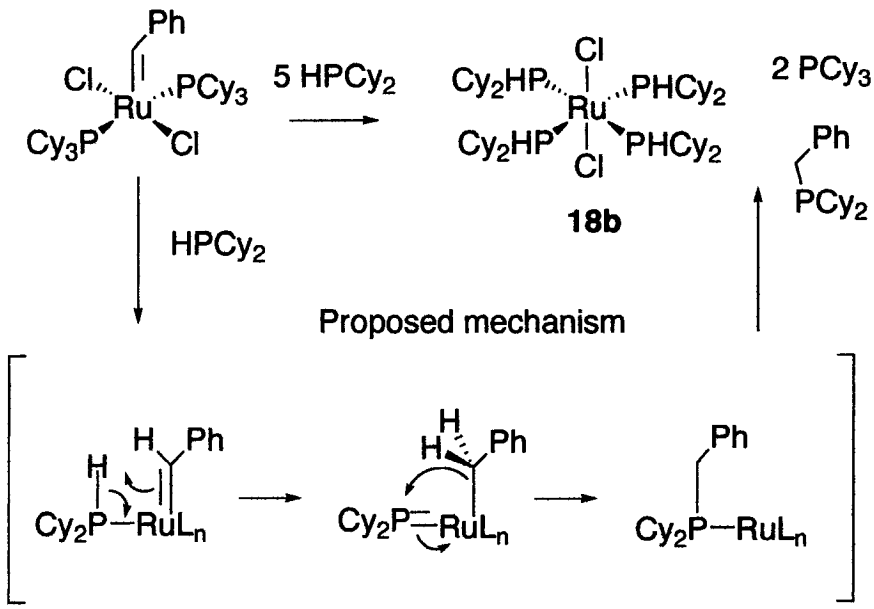

Figure 5.8. Synthesis of **18b** from Grubbs catalyst.

In situ ^{31}P NMR analysis reveals a singlet assigned to trans isomer **18b** at δ 14.56, free PCy_3 ligand at δ 3.22 ppm, and $P(CH_2Ph)Cy_2$ at δ 11.24 ppm (ratio 4:2:1). Formation of $P(CH_2Ph)Cy_2$ can be rationalized as the hydrophosphination product of the benzylidene ligand and one $HPCy_2$. The assignments of **18b**, PCy_3, and $P(CH_2Ph)Cy_2$ (synthesized separately by reaction of benzyl bromide with $HPCy_2$) were confirmed with the NMR spectra of the authentic compounds.

Of note, mostly the trans product **18b** (>95%) forms in this reaction, which contrasts with the formation of predominantly cis **18a** from the reaction of $HPCy_2$ with $RuCl_2(PPh_3)_3$ (Figure 5.3). The clean transformation from Grubbs catalyst to **18a** could lead to new and improved tandem catalytic protocols, such as highly selective tandem metathesis/ketone transfer hydrogenation.

5.3 Transfer hydrogenation catalysis by 18a/b-23.

The complexes **18a/b-23** were tested for catalytic activity in transfer hydrogenation of acetophenone (Substrate:Base:Catalyst = 1000:20:1). Only $HPCy_2$ complexes **18a/b, 21,** and **22** were highly active. Furthermore, catalysis under H_2 atm prevents catalyst deactivation (Figure 5.9).

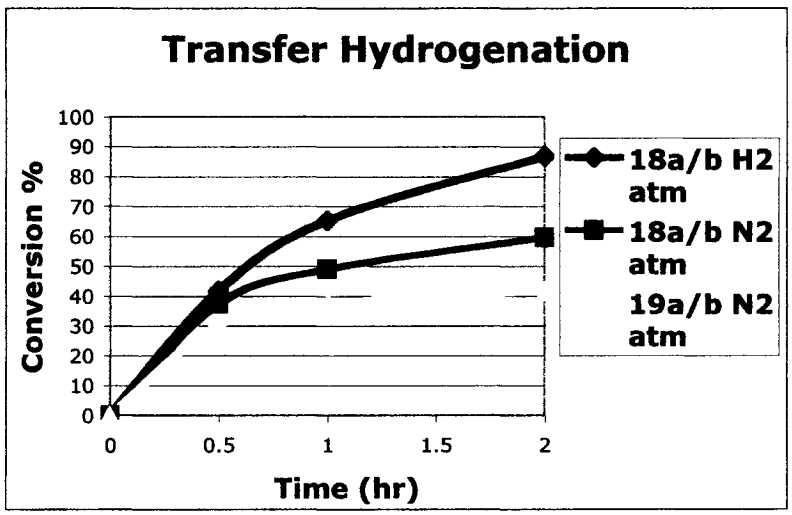

Figure 5.9. Plot of transfer hydrogenation activity for **18a/b** under H_2 and N_2 atmosphere, and **19a/b** under N_2 atmosphere.

Complexes **20a/b,** based on the PH_2Ph ligand, show no catalytic activity. The complex may deactivate rapidly under the highly basic conditions used. $PHPh_2$ based complex **19a/b** initially shows the same high activity as $PHCy_2$ complex **18a/b** (Figure 5.9), but deactivates more readily at moderate conversions. Deactivation could be due to low stabilization of phosphido intermediates by the the weakly-donating $HPPh_2$ ligand. Deactivation for **19a/b** was observed under both N_2 and H_2 atmospheres. Pincer complex **23** showed no catalytic activity, probably due to the constrained geometry.

The catalytic activities observed for the most active complexes, **18a/b**, **21**, and **22,** were virtually identical, suggesting that the dichloride complex **18a/b** forms monohydride **21** rapidly, and that **21** goes on to form cis dihydride **22** (Figure 5.10). Deactivation occurs under N_2 atmosphere for all three. Hydrogen appears to play a role in the stabilization of the catalytic system, as less deactivation occurred under one atmosphere of hydrogen.

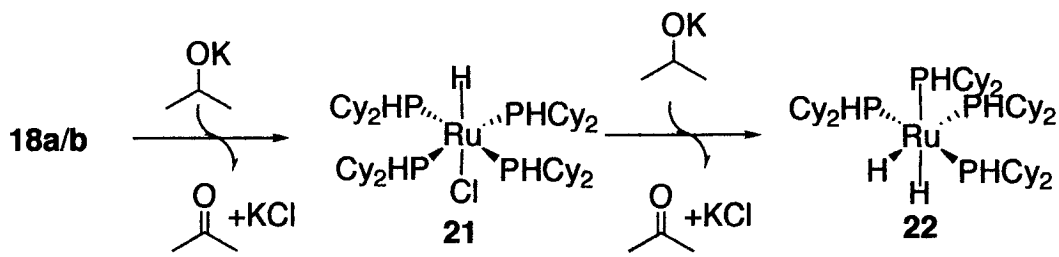

Figure 5.10. Transformation of the catalytic precursors **18a/b** and **21** to dihydride **22** in basic isopropyl alcohol.

By analogy to the Noyori and Bäckvall systems,[4,7] dihydride **22** may function as the active species in this system. A critical function of H_2 may be

regeneration of a $Ru(H)(PHR_2)$ species by addition to the $Ru\text{-}PR_2$ intermediate. An outer sphere mechanism (Figure 5.3) would render more hindered substrates more easily reducible, as the substrates are further from the metal center than in an inner sphere mechanism. Benzophenone, known to be a difficult substrate for inner sphere catalysts due mainly to steric bulk (see Chapter 3), was used as a substrate for **18a/b** catalyzed transfer hydrogenation. An initial experiment using precatalyst **18a/b** (without pre-treatment), led to very high conversions in 2 hours (80% conversion, S:B:C = 1000:20:1), which is an order of magnitude higher than that for pincer complex **3**. The activity of **18a/b** is virtually identical when comparing for benzophenone and acetophenone reduction, while the activity of the pincer catalyst **7** and $RuH_2(PPh_3)_3$ is strongly substrate dependant. The Noyori catalyst, likewise, showed little discrimination between acetophenone and benzophenone. This may be a common characteristic of catalysts operating by outer-sphere coordination of substrate.[14]

5.4. Conclusions.

This chapter described the study of $RX_2(PHR_2)$ complexes in catalysis. $HPCy_2$ complex **18a/b** was highly active in transfer hydrogenation catalysis, presumably due to the higher basicity of $HPCy_2$ compared to the primary and secondary aryl phosphines in **19a/b** and **20a/b**. The high affinity of $HPCy_2$ for ruthenium also enabled clean transformation of Grubbs catalyst to **18b**,

potentially opening the way to tandem metathesis-hydrogenation catalysis with $HPCy_2$ as a ligand.

References

(1) Kirby, A. J.; Hartwell, E.; Hodgson, D. R. W. *J. Am. Chem. Soc* **2000**, *122*, 9326.
(2) Noyori, R.; Ohkuma, T. *Angew. Chem., Int. Ed. Engl.* **2001**, *40*, 40.
(3) Noyori, R.; Ohkuma, T.; Ooka, H.; Ikariya, T. *J. Am. Chem. Soc* **1995**, *117*, 10417.
(4) Noyori, R.; Sandoval, C. A.; Ohkuma, T.; Muñiz, K. *J. Am. Chem. Soc* **2003**, *125*, 13490.
(5) Rosenberg, L.; Westmore, J. B.; Hooper, T. S.; Willett, G. D.; Fisher, K. J. *Organometallics* **2002**, *21*, 5688.
(6) Abdur-Rashid, K.; Lough, A. J.; Morris, R. H. *Organometallics* **2000**, *19*, 2655.
(7) Morris, R. H.; Abdur-Rashid, K.; Clapham, S. E.; Hadzovic, A.; Harvey, J. N.; Lough, A. J. *J. Am. Chem. Soc* **2002**, *124*, 15104.
(8) Crabtree, R. H. *The Organometallic Chemistry of the Transition Metals.* Wiley-Interscience: Toronto, 1994.
(9) Tolman, C. A.; Faller, J. W. *Homogeneous Catalysis with Metal Phosphine Complexes.* Plenum Press: New York, 1983.
(10) Poe, A. J.; Babij, C.; Chen, L.; Koshevoy, I. O. *Dalton Trans.* **2004**, 833-838.
(11) Blaser, H. U.; Schnyder, A.; Indolese, A. F.; Studer, M. *Angew. Chem. Int. Ed.* **2002**, *41*, 3668.
(12) Noels, A. F.; Jan, D.; Delaude, L.; Simal, F.; Dimonceau, A. *Can. J. Chem.* **2001**, *79*, 529.
(13) Simpson, R. H.; Blake, A. J.; Champness, N. R.; Forder, R. J.; Frampton, C. S.; Frost, C. A.; Reid, G. *Dalton Trans.* **1994**, 3377.
(14) Noyori, R.; Hashiguchi, S. *Acc. Chem. Res.* **1997**, *30*, 97, and references therein.

CHAPTER 6

Conclusions and Future Considerations

This thesis discussed work in the related themes of mechanistic studies and new ligand design in homogeneous ruthenium catalysis. Mechanistic understanding of ruthenium pincer catalyzed transfer hydrogenation is described in Chapter 3. During the pretreatment of $RuCl(\eta^3\text{-dcpx})PPh_3$ (**7**), several different hydride products were observed. The formation of a catalytically active coordinatively unsaturated η^2-bound PC(H)P intermediate was proposed on the basis of the kinetics and in situ NMR analysis. This highlights the value of understanding the possible formation of a catalytically active η^2-bound PC(H)P species in other ruthenium pincer catalyzed reactions.

In order to utilize the potential of Ru(II) complexes in homogeneous catalysis, it is desirable to minimize the formation of trichloride-bridged dinuclear structures. Use of alternative anionic ligands in place of the chloride donors can possibly inhibit such bimolecular deactivation. Novel ligands incorporating pyrrole derivatives bearing two imidazolium groups were designed and synthesized for potential catalytic applications, but no metal complexes could be generated. Related ligands have been proposed which may enable synthesis of metal complexes of pyrrole-NHC chelates.

Our interest in new ligands useful for catalytic applications led us to test secondary phosphine complexes of ruthenium in transfer hydrogenation catalysis. The bulky secondary phosphine ligand in $RuCl_2(HPCy_2)_4$ (**1 9**),

conferred high activity in transfer hydrogenation. Of interest, this complex could also be generated from the Grubbs catalyst, suggesting potential tandem metathesis-hydrogenation applications. Future work could focus on understanding the mechanism of transfer hydrogenation catalysis by ruthenium-$HPCy_2$ complexes.